NIH Public Access
Author Manuscript
Dev Dyn. Author manuscript; available in PMC 2016 January 01.

Published in final edited form as:
Dev Dyn. 2015 January ; 244(1): 69–85. doi:10.1002/dvdy.24180.

A molecular atlas of *Xenopus* respiratory system development

Scott A. Rankin[1], **Hong Thi Tran**[3], **Marcin Wlizla**[1], **Pamela Mancini**[1], **Emily T. Shifley**[1,#], **Sean D. Bloor**[1], **Lu Han**[1], **Kris Vleminckx**[3], **Susan E. Wert**[2], and **Aaron M. Zorn**[1,*]

[1]Division of Developmental Biology, Perinatal Institute, Cincinnati Children's Hospital, and the Department of Pediatrics, College of Medicine University of Cincinnati, Cincinnati OH 45229

[2]Division of Pulmonary Biology, Perinatal Institute, Cincinnati Children's Hospital, and the Department of Pediatrics, College of Medicine University of Cincinnati, Cincinnati OH 45229

[3]Department for Biomedical Molecular Biology, Ghent University, B-9052 Ghent Belgium

Abstract

Background—Respiratory system development is regulated by a complex series of endoderm – mesoderm interactions that are not fully understood. Recently *Xenopus* has emerged as an alternative model to investigate early respiratory system development, but the extent to which the morphogenesis and molecular pathways involved are conserved between *Xenopus* and mammals has not been systematically documented.

Results—In this study we provide a histological and molecular atlas of *Xenopus* respiratory system development, focusing on Nkx2.1^{+} respiratory cell fate specification in the developing foregut. We document the expression patterns of Wnt/β-catenin, FGF, and BMP signaling components in the foregut and show that the molecular mechanisms of respiratory lineage induction are remarkably conserved between *Xenopus* and mice. Finally, using a number of functional experiments we refine the epistatic relationships between FGF, Wnt and BMP signaling in early *Xenopus* respiratory system development.

Conclusions—We demonstrate that *Xenopus* trachea and lung development, before metamorphosis, is comparable at the cellular and molecular levels to embryonic stages of mouse respiratory system development between E8.5 to E10.5. This molecular atlas provides a fundamental starting point for further studies using *Xenopus* as a model to define the conserved genetic programs controlling early respiratory system development.

Keywords

respiratory system; lung; trachea; *Xenopus*; development; Nkx2.1; respiratory epithelium; specification

*correspondence: Aaron.zorn@cchmc.org.
#Present address: Department of Biological Sciences, Northern Kentucky University, Highland Heights KY 41076

NIH-PA Author Manuscript
NIH-PA Author Manuscript
NIH-PA Author Manuscript

NIH-PA Author Manuscript

NIH-PA Author Manuscript

NIH-PA Author Manuscript

Introduction

The evolution of vertebrate lungs was an essential adaptation to air breathing in the terrestrial environment. The epithelial lining of the respiratory system is comprised of a number of different epithelial cell types including pneumocytes in the aveolar regions that facilitate gas exchange and secrete surfactant proteins enabling the lungs to inflate. In the trachea and large airways, ciliated and secretory cells are critical for defense against pathogens and keeping the lungs clear for breathing. The billions of epithelial cells lining the mammalian trachea and lungs originate from just a few hundred respiratory progenitor cells in the ventral foregut endoderm of the early embryo, which are formed around 28 days of human gestation and at embryonic day (E) 9.5 in mouse development (Morrisey and Hogan, 2010). Knowledge of the molecular mechanisms orchestrating respiratory system organogenesis informs our understanding of human congenital lung defects such as pulmonary dysplasia and tracheo-esophageal fistula (Herriges and Morrisey, 2014; Whitsett et al., 2011), and provides insight into strategies to differentiate human respiratory tissue from pluripotent stem cells which ultimately may be used for regenerative medicine (Huang et al., 2014; Longmire et al., 2012; Wong and Rossant, 2013).

To date, our understanding of early respiratory system development has come primarily from genetic studies in mice. Specification of the respiratory progenitors can first be identified in the mouse by the expression of the homeodomain transcription factor Nkx2.1 (TTF-1) in a subset of the ventral foregut endoderm around E9.5 of development (Lazzaro et al., 1991). This induction of Nkx2.1 expression occurs concomitantly with the down-regulation of the transcription factor Sox2, which is initially expressed throughout the foregut epithelium and then becomes restricted to the dorsal foregut epithelium that gives rise to the lining of the esophagus (Hines and Sun, 2014; Morrisey and Hogan, 2010; Ornitz and Yin, 2012).

Studies in mice have implicated paracrine FGF, Wnt/β-catenin, and BMP signals from the surrounding mesenchyme as being critical for induction of the $Nkx2.1^{+}$ respiratory lineage (Hines and Sun, 2014; Morrisey and Hogan, 2010; Ornitz and Yin, 2012). Explant culture studies with mouse embryonic foregut tissue suggest that between E8 and E9, FGF signals from the cardiogenic mesoderm segregate foregut cells into lung, liver, and pancreas lineages in a dose-dependent fashion with the highest levels of FGF promoting lung fate (Serls et al., 2005). It is postulated that multiple redundant FGF ligands mediate this process *in vivo*, but this remains to be genetically validated. Shortly after this putative FGF signal, redundant Wnt2 and Wnt2b ligands expressed in the splanchnic mesoderm signal to the ventral foregut endoderm to induce respiratory progenitors. The combined deletion of *Wnt2* and *Wnt2b*, or the conditional deletion of the canonical Wnt-effector β-*catenin* from the foregut epithelium, results in a failure to induce Nkx2.1 expression and respiratory system agenesis (Goss et al., 2009; Harris-Johnson et al., 2009). In addition ectopic activation of β-catenin in the foregut epithelium results in expanded Nkx2.1 expression, suggesting that canonical Wnt signaling is necessary and sufficient to induce lung fate (Goss et al., 2009; Harris-Johnson et al., 2009).

NIH-PA Author Manuscript

NIH-PA Author Manuscript

NIH-PA Author Manuscript

BMP ligands from the ventral mesoderm appear to cooperate with Wnt2/2b to promote respiratory fate. Conditional deletion of the type I BMP receptors genes *Bmpr1a* and *Bmpr1b* from the mouse foregut epithelium results in tracheal agenesis and signaling through these receptors is also required for the ectopic Nkx2.1 expression induced by hyperactive β-catenin (Domyan et al., 2011). Mechanistically, BMP signaling appears to act primarily by down-regulating expression of Sox2, which is inhibitory to *Nkx2.1* expression (Domyan et al., 2011). The balance between ventrally expressed BMP ligands and the secreted BMP-antagonist Noggin from the dorsal notochord results in differential phosphorylation and activation of the BMP effectors Smad1/5/8 across the dorsal-ventral (D–V) axis of the E9.5 foregut, with phospho-Smad1/5/8 (pSmad1) levels being highest in the ventral foregut and low or absent in the dorsal foregut. This D–V patterning of the foregut is critical for the proper separation of the trachea and esophagus and defects in this process can result in trachea-esophageal fistulas and in some cases agenesis of the trachea or esophagus (Fausett and Klingensmith, 2012; Que et al., 2006).

Although mouse genetics have been invaluable in identifying the critical role of the aforementioned paracrine signaling factors, how the different pathways and their downstream effectors interact in a complex regulatory network remains to be fully elucidated. One of the challenges has been the difficulty working with early mouse embryos and the limited material available from compound mutants. Recently the frog *Xenopus* has emerged as an alternative model to investigate early respiratory development (Rankin et al., 2012; Shifley et al., 2012; Wang et al., 2011; Yin et al., 2010). The experimental advantages of the abundant and large externally developing *Xenopus* embryos make them well suited to study complex signaling pathways (Blitz et al., 2006; Harland and Grainger, 2011) and are therefore also a promising model to examine the gene regulatory networks governing early respiratory system development. However the extent to which respiratory system development is conserved between *Xenopus* and mammals has not yet been systematically examined.

In this study we provide a histological and molecular atlas of *Xenopus* respiratory system development with a focus on the stages when lung and trachea epithelia are specified in the embryonic foregut. Our analysis reveals that early respiratory system development in *Xenopus* (prior metamorphosis) is very similar to the embryonic phase of mouse lung and trachea development between E8.5 to E10.5. We document the spatial expression of key components of the Wnt/β-catenin, FGF, and BMP pathways in the *Xenopus* foregut and confirm that the molecular mechanisms of respiratory system development are remarkably conserved between *Xenopus* and mice. Finally using both loss-of-function and gain-of-function experiments we resolve the epistatic relationships between the FGF, Wnt, and BMP pathways during D–V pattering of the foregut and specification of $Nkx2.1^{+}$ respiratory progenitors in *Xenopus*. This molecular atlas provides a valuable reference for further studies using *Xenopus* as a model to elucidate the conserved genetic programs controlling early respiratory system development.

NIH-PA Author Manuscript

NIH-PA Author Manuscript

NIH-PA Author Manuscript

Results and Discussion

Histological atlas of Xenopus respiratory system development

To document respiratory system development in *Xenopus laevis* we first performed a histological analysis on a range of developmental stages from tailbud embryos to metamorphosis (Fig. 1). By 40 hours post-fertilization (hpf), at Nieuwkoop and Faber stage 32 (NF32) (Nieuwkoop and Faber, 1994), the foregut is a simple oval-shaped endoderm tube surrounded by lateral plate mesoderm (Figure 1C–E) without any histological evidence of lung bud formation. Ten hours later at NF35 the foregut has undergone considerable morphogenesis (Fig.1F–H). At this stage the anterior end of the developing respiratory system can first be detected as a laryngo-tracheal groove protruding ventrally from the endodermal floor of the pharynx (Fig.1F). More posteriorly the foregut becomes constricted in the middle as distinct dorsal esophageal and ventral tracheal tubes begin to separate (Fig. 1G). The first indication of lung buds can be detected at NF35 as bilateral evaginations from the ventral foregut epithelium (Fig.1H). Approximately one day later, at NF42 (~80 hpf), the foregut tube has completely separated into an esophagus lined by stratified epithelium and a trachea lined by a single-layered epithelium, which bifurcates into the two primary lung bud bronchi (Fig.1I–K). At this stage the esophagus and respiratory system are surrounded by a loose mesenchymal layer, which is more condensed at the distal tips of the lung buds. By the beginning of metamorphosis at NF52 (~19 days pf) (Fig.1L–N) the lung buds have grown 2–3 times in size (1–2 mm in length) but are still simple sac-like structures, comprised of a single layer of epithelium surrounded by a thin layer of mesenchyme, with the pulmonary arteries and pulmonary veins running along the lateral and medial lengths of the lung buds respectively (Fig. 1N) (Bartel and Lametschwandtner, 2000). Studies indicate that these simple larval lungs are functional at this stage as tadpoles can be observed taking air into their lungs from the surface starting around NF46 (Feder et al., 1984; Rose and James, 2013).

As development progresses, a striking difference between *Xenopus* and mouse lung morphogenesis becomes evident. Amphibian lungs, including those of *Xenopus*, do not undergo the stereotypical branching morphogenesis characteristic of mammalian fetal lungs (Waterman, 1939). Rather during metamorphosis, between NF54 to NF65, *Xenopus* lung buds undergo a septation process (Nieuwkoop and Faber, 1994; Rose and James, 2013), where epithelial covered muscular projections or “septa” emerge from the lung walls to generate a series of peripheral alveolar sacs (Fig. 1B, P, Q). Septation proceeds in a caudal to cranial fashion progressively expanding the epithelial surface area available for oxygen exchange, with pulmonary blood vessels within and at the base of the septa (Fig. 1 O–Q; data not shown). During this period the mesenchyme surrounding the trachea and lung buds differentiates into a thin smooth muscle layer, with hyaline cartilage plates in the walls of the trachea and main bronchi similar to the mammals (Fig. 1O)(Rose and James, 2013). Unlike in mammals however, cartilage nodules are also present within proximal lung buds (Fig. 1P,Q). For a more detailed description of frog lung bud septation during metamorphosis see: (Bartel and Lametschwandtner, 2000; Nieuwkoop and Faber, 1994; Rose and James, 2013; Waterman, 1939). In summary, the histology and morphogenesis of

NIH-PA Author Manuscript

NIH-PA Author Manuscript

NIH-PA Author Manuscript

early *Xenopus* respiratory system development, prior to metamorphosis, is strikingly similar to mouse lung development between E8.5 - E10.5, before branching morphogenesis.

Histology of the adult Xenopus lung

To provide a context for our embryological studies we present a brief overview of adult *Xenopus* lung histology in Figure 2, for more detailed descriptions see: (Meban, 1973; Okada et al., 1962; Smith and Rapson, 1977; Wiechmann and Wirsig-Wiechmann, 2003). The *Xenopus* trachea connecting the oral cavity to the primary bronchi is quite short relative to mammals. The adult *Xenopus* lung is a single multi-chambered sac divided by muscular septa into a series of bronchiole chambers surrounding a central airway that extends down the length of the lung (Fig. 2A, A', H–J). Major bronchi are further divided into smaller alveoli by thinner secondary and tertiary septa, the tips of which contain smooth muscle bundles surrounded by collagen (Fig. 2C", D). Cartilage nodules are found in the walls of the trachea and main bronchi (Fig. 2A, B, B'), as well as at the ends of the major septa in the proximal region of the conducting airway (Fig. 2C, C'). The outer wall of the lung consists of several relatively thin layers of muscle and connective tissue (Fig. 2A, B). Major pulmonary vein and artery run longitudinally down the length of lung along the central airway, with smaller pulmonary vessels frequently observed in the tips of the alveolar septa (Fig. 2C"). The internal surface of the lung, including the alveoli septa are lined by endoderm-derived thin squamous epithelium tightly apposed to endothelial cells of the sub-epithelial capillary network (Fig. 2B–F). Previous ultra structure studies of the air-blood interface indicate that the respiratory epithelium cells in *Xenopus* are a single type of pneumocyte, which have hybrid features of both alveolar type I and alveolar II type cells in mammals, which absorb oxygen and secrete surfactant respectively (Meban, 1973). In situ hybridization confirmed expression of the type II cell marker *surfactant protein C* (*sftpc*) in the cell body of many epithelial cells lining the adult *Xenopus* lung (Fig. 2G). Because in situ hybridization cannot reliably detect transcripts in the thin cytoplasmic extensions of the pneumocytes it is unclear whether all the epithelial cells express *sftpc* and it remains possible that at the molecular level there may be different pneumocytes subtypes.

Molecular characterization of the developing respiratory epithelium in Xenopus

We next documented the expression profile of genes in the developing *Xenopus* respiratory epithelium focusing on genes that have important roles in mammalian respiratory system development. In situ hybridization at NF32 shows that mRNA encoding the transcription factors Foxa2, Foxa1, and Sox2 as well as the secreted signaling molecule Shh are expressed throughout the entire foregut endoderm (Fig. 3A–I; data not shown) (Yin et al., 2010). The pan-foregut expression of these genes is similar to that observed in E8-E9 mouse embryos, where Foxa1 and Foxa2 act as key 'pioneering' factors known to regulate epigenetic chromatin status and competence of the foregut epithelium (Zaret and Carroll, 2011). The first molecular indication of the respiratory lineage is the expression of the homeobox gene *nkx2.1* in the ventral foregut starting at NF33 in *Xenopus* (Fig. 3N) (Hollemann and Pieler, 2000; Small et al., 2000) and at E9.5 in mice (Lazzaro et al., 1991). As in mammals, *Xenopus nkx2.1* is also expressed in the thyroid and forebrain. In mice surfactant gene expression (*Sftp-a*, *Sftp-b*, *Sftp-c*, and *Sftp-d*) are the earliest definitive markers of the respiratory epithelium, with *Sftpc* detectable at E11(Wert et al., 1993). *Xenopus* also

NIH-PA Author Manuscript

NIH-PA Author Manuscript

NIH-PA Author Manuscript

contains four *sftp* genes (Xenbase.org), and as previously described, *sftpc* and *sftpb* mRNA are expressed throughout the respiratory epithelium beginning at NF37/38 (Fig. 3V–Y) (Hyatt et al., 2007; Yin et al., 2010), but are undetected in any other tissues indicating that they are unambiguous marker of respiratory epithelium at these stages. In mice, Foxa1, Foxa2, Nkx2.1, and Gata6 have been implicated in transcriptional activation of *Sftp-c* (Maeda et al., 2007), and likewise all of these factors were expressed in the *sftpc*$^{+}$ epithelium of the developing *Xenopus* lung buds (Fig. 3; data not shown).

We next assayed later stages (NF42-59) to determine if there were any molecular differences in proximal-distal character of the *Xenopus* lung bud epithelium. During the pseudo-glandular stages of mouse lung development (E12-E16) the respiratory epithelium becomes regionalized with *Sox2* being re-expressed in the trachea and proximal upper airway (in addition to the esophagus), whereas *Sox9* and *Nkx2.1* expression becomes restricted to the distal tips of the lung buds (Morrisey and Hogan, 2010). Similar to mice we observed a progressive restriction of *nkx2.1* to the distal lung tips (Fig. 3O–Q) and *sox2* was detected, albeit weakly, in the trachea and proximal main bronchi (Fig. 3L). In contrast, *sox9* did not exhibit distally restricted expression pattern like in mouse. Initially *sox9* is not expressed in the lung epithelium (NF35) and weak expression was first detected in the lung buds at NF42 (Fig. 3 R, S). Between NF49-59, during the period of lung bud septation, the entire lung epithelium robustly expressed *sox9* similar to *sftpc* (Fig. 3T, U). Interestingly, a recent report on the role of Sox9 in lung branching morphogenesis compared early *Xenopus* and mouse lung buds. This study, which only examined *Xenopus* up to NF 42, concluded that *Xenopus* lung buds did not express *sox9*, and suggested that this might explain the lack of branching morphogenesis in *Xenopus* (Chang et al., 2013). This conclusion probably needs to be reexamined in light of our findings here that the *Xenopus* lungs do indeed express *sox9* during septation.

Overall, our data indicate that the developing respiratory epithelium in *Xenopus* exhibits dynamic temporal and spatial gene expression patterns similar to that observed in early mouse embryo between E8.5-E10.5.

Dorsal-ventral patterning of the Xenopus foregut: tracheal-esophageal separation

A key aspect of early mammalian respiratory development is the D–V patterning of the foregut with the progressive restriction of Sox2 expression to the dorsal foregut and the induction of Nkx2.1^{+} respiratory progenitors in the ventral foregut, which ultimately separate into the esophagus and trachea respectively. To examine this process in detail we performed immunostaining of Nkx2.1 and Sox2 protein in the *Xenopus* foregut from stages NF32 to NF42 (Fig. 4).

At NF32, prior to induction of the respiratory lineage Nkx2.1 was undetectable, while Sox2 was observed throughout the foregut epithelium, with stronger expression in the dorsal region (Fig. 4A–C). Serial sections along the A–P axis shows that Nkx2.1^{+} nuclei are first weakly observed at NF33 coincident with initial thickening of the ventral foregut epithelium and the down regulation of Sox2 (Fig. 4D–F). By NF34, Nkx2.1 protein was robustly expressed in the laryngo-tracheal groove, a ventral protrusion in floor of the pharynx, in the presumptive trachea and in bilateral endodermal thickenings where the lungs will form (Fig.

NIH-PA Author Manuscript

NIH-PA Author Manuscript

NIH-PA Author Manuscript

4G–I). This expression is clearly distinct from the more anterior Nkx2.1$^+$ thyroid domain (Fig. 3N). At this stage Nkx2.1 and Sox2 become mutually exclusive with Sox2 being restricted to the dorsal foregut epithelium. This arrangement of Sox2/Nkx2.1 in the NF33/34 *Xenopus* foregut is strikingly similar to that found in mouse at E9.5 (Fig. 4P). At NF35/36 Nkx2.1 was detected in the region of the ventral foregut that will give rise to the trachea and in the nascent lung buds evaginating from the ventral foregut, whereas Sox2$^+$ epithelium lines the pharynx, presumptive esophagus and more posteriorly the future stomach (Fig.4J–L). In mice another marker of the developing esophageal epithelium is p63 and similarly *Xenopus* p63 was expressed in a subset of dorsal foregut epithelium (Fig. 4Q, R). Finally at NF42, consistent with the H&E histology (Fig.1), the Nkx2.1$^+$ trachea was completely separated from the Sox2$^+$ esophagus (Fig. 4M–O). This timing of trachea and esophagus separation in *Xenopus* between stages NF34 and NF42 is roughly 35 hours, compared to the 48 hours that this process takes in mice between E9.5 and E11.5.

Throughout this period the foregut epithelium is surrounded by lateral plate mesoderm (lpm) expressing Foxf1 protein (Fig.4), a forkhead transcription factor essential for differentiation and proliferation of the developing splanchnic mesenchyme in *Xenopus* (Tseng et al., 2004). Foxf1 plays a number of important roles in mammalian lung development and Foxf1$^{+/-}$ heterozygous mutations in mice and humans leads to Alveolar Capillary Dysplasia with Misalignment of Pulmonary Veins, a lethal congenital condition (Kalinichenko et al., 2002; Mahlapuu et al., 2001). Some lpm cells surrounding the ventral foregut also express markers of cardiac mesoderm (*gata4* and *gata6*) and endothelial cells (*flk1* and *etv2*) (data not shown), consistent with the closely coordinated development of the pulmonary vasculature and the heart.

Morphogenesis of the respiratory system in mice is accompanied by extensive remodeling of the extracellular matrix (ECM), which can also impact diffusible ligands signaling between the foregut mesenchyme and epithelium (Shannon et al., 2003). We therefore analyzed the ECM in the *Xenopus* foregut at NF33-35. Immunostaining showed a Fibronectin-rich ECM in the mesenchyme surrounding the foregut epithelium, with a basement membrane containing heparin sulfate proteoglycan (pan-HSPG) and Laminin-α1 separating the endoderm and mesoderm layers (Fig. 5A–L). Chondroitin sulfate proteoglycans (CSPG), another major ECM component required for lung bud morphogenesis in mouse (Shannon et al., 2003) was highly enriched around the ventral foregut and nascent lung buds (Fig.5M–O). We noticed that in the CSPG-rich region where the primary lung buds evaginate from ventral foregut, the basement membrane was partially disrupted (yellow arrows in Fig.5D'-F', K). This is similar to what has been reported during outgrowth of the embryonic liver bud where it is thought that endothelial cells regulate basement membrane breakdown (Matsumoto et al., 2001).

Expression of Wnt pathway components during Xenopus respiratory specification

In mice Wnt2 and Wnt2b signaling via β-catenin is essential for respiratory fate (Goss et al 2009; Harris-Johnson et al 2009). We recently found that Wnt2 and Wnt2b, expressed in the lpm surrounding the ventral foregut endoderm (Fig. 6A,B), are also redundantly required for *Xenopus* lung specification (Rankin et al., 2012), but it is unknown in any species which

NIH-PA Author Manuscript

NIH-PA Author Manuscript

NIH-PA Author Manuscript

Wnt receptors or Tcf/Lef transcription factors mediate Wnt2/2b signaling. To begin to address this we performed a systematic expression analysis of Wnt pathway components during *Xenopus* respiratory specification stages (NF30-35) using *in situ* hybridization and by analyzing published expression patterns in Xenbase.org. We show the data for stage NF34/35, which is immediately after initial respiratory specification so that we can use the thickening epithelium as a landmark of the lung region, however all of the genes we present were similarly expressed during induction at NF30-33, albeit more weakly in some cases.

Of 10 frizzled Wnt-receptor genes (*fzd1 – fzd10*), only *fzd4*, *fzd6* and *fzd7* were robustly expressed at the right time and place to be involved in lung specification. *Fzd4* was enriched in both the ventral foregut endoderm as well as ventral lpm (Fig. 6D, D'), whereas *fzd7* was only detected in the ventral lpm (Fig. 6C), and *fzd6* was ubiquitously expressed throughout the anterior embryo, including the foregut endoderm and lpm (data not shown) (Zhang et al., 2011). In addition *fzd2* was ubiquitously expressed at low levels in the endoderm and mesoderm during early tailbud stages, but was not detectable in the NF32-35 foregut, whereas *fzd8* was expressed in the lung buds only after specification at NF42 (data not shown and Xenbase.org). We note that *fzd2, fzd4, fzd6, fzd7, and fzd8* have all been knocked out in mouse, and none appear to have a respiratory phenotype, suggesting functional redundancy. In canonical Wnt signaling Lrp5 and Lrp6 co-receptors bind to Wnt ligands and Fzd receptors stimulating the phosphorylation of the Lrp5/6 cytoplasmic domain to recruit Axin and stabilize β-catenin (reviewed in (Niehrs, 2012). In situ hybridization revealed that *lrp5, lrp6* and *axin2* were robustly expressed throughout the foregut mesoderm and endoderm, consistent with mediating Wnt2/2b signaling (Fig. 6E–G'), whereas *axin1* transcripts were not detected in the foregut region at this stage (data not shown). R-spondin genes (*rspo*) encode another family of secreted proteins that promote Wnt signaling by protecting Fzd receptors from degradation (Niehrs, 2012), and in mice *Rspor2* is important for laryngeal-tracheal and lung development (Bell et al., 2008). Consistent with the possibility of a similar role in *Xenopus* we found that *rspo2* transcripts are enriched in the ventral lpm and foregut endoderm, whereas *rspo1* and *rspo3* were undetectable (Fig. 6H–J').

Of the four Tcf/Lef family members *tcf1* (also known as t*cf7*) was uniquely enriched in both the ventral foregut endoderm and ventral lpm (Fig. 6K) at the time of respiratory specification. *Tcf3* and *lef1* were ubiquitously expressed throughout the anterior portion of the embryo, including the foregut endoderm and lpm, whereas *tcf4* was only detected in the nervous system and posterior portion of the embryo at this stage (Fig. 6L–N'). Thus, *tcf1*, *tcf3*, and *lef1* are all expressed at the right time and place to regulate gene expression downstream of Wnt2/2b during respiratory specification.

To directly monitor which cells in the foregut are responding to canonical Wnt/β-catenin signaling during respiratory system development we analyzed a transgenic *Xenopus tropicalis* reporter line *Tg(7xtfc:degfp)*, which harbors 7 copies of the consensus Tcf/Lef DNA-binding site driving expression of destabilized EGFP (Tran et al., 2010). Co-staining of embryos using EGFP and Nkx2.1 (or Sox2) antibodies revealed that EGPF expression was first weakly detectable in the ventral foregut at NF32 prior to Nkx2.1 expression (Fig. 7A–A') when all of the foregut epithelium expresses Sox2 (Fig. 7B, B'). By NF33 robust EGFP expression was detected in the Nkx2.1^{+} ventral epithelium, coincident with the down

NIH-PA Author Manuscript

NIH-PA Author Manuscript

NIH-PA Author Manuscript

regulation of Sox2 (Fig. 7B–F'). We also detected reporter activity in the surrounding lpm. From NF35-42 EFGP was strongly expressed in the developing trachea and lung buds (Fig. 7G–L') indicating that these tissues are experiencing prolonged Wnt signaling. In addition EGFP expression was detected in the ventral portion of the esophageal tube and in the stomach at NF42 (Fig. 7J'-L').

Together these data identify the candidate Wnt-receptors and Tcf/Lef transcription factors that are likely to mediate Wnt2/2b signaling during *Xenopus* respiratory system induction. Moreover the *fzd* expression and the transgenic reporter demonstrate that both the epithelium and the mesenchyme respond to canonical Wnt signaling. This is consistent with findings in mice where in addition to its role in respiratory specification Wnt2 also promotes lung bud outgrowth and pulmonary smooth muscle differentiation (Goss et al., 2011).

Expression of FGF pathway components during Xenopus respiratory specification

FGF signaling is well known to regulate murine lung bud outgrowth and branching morphogenesis (Ornitz and Yin, 2012), but the role of FGFs in specifying mammalian respiratory progenitors is obscure. Mouse explant experiments suggest that FGF signaling promotes Nkx2.1$^+$ lung fate (Serls et al., 2005), and FGF2, FGF7, and FGF10 have been used to direct respiratory differentiation in mouse and human ES cells *in vitro* (Huang et al., 2014; Longmire et al., 2012; Wong and Rossant, 2013). But this remains to be genetically validated *in vivo* and it is postulated that multiple redundant ligands are involved. Candidates include *Fgf1*, *Fgf2, Fgf7, Fgf9* and *Fgf10* all of which are expressed in the mesenchyme surrounding the mouse foregut at E8-E10. However all of the individual and compound *Fgf* gene knockouts described in mice to date still specify Nkx2.1$^+$ lung progenitors, although *Fgf9* and *Fgf10* are clearly essential for lung bud outgrowth, branching morphogenesis and proper differentiation of the lung epithelium and mesenchyme (Sekine et al., 1999; Yin et al., 2011; Yin et al., 2008).

Inhibitor studies in *Xenopus* provided the first *in vivo* evidence that FGF signaling is essential for specification of Nkx2.1$^+$ respiratory progenitors (Rankin et al., 2012; Shifley et al., 2012; Wang et al., 2011), however the specific ligands involved have not been characterized. Analyses of published expression patterns suggested that, like in mice, *fgf1*, *fgf2*, *fgf7*, *fgf9* and *fgf10* are the best candidates (Lea et al., 2009), but their expression in the foregut has not been examined in detail. In situ hybridization showed that while *fgf1* and *fgf2* were expressed in the anterior lpm during pattering stages from NF13-25 they were only weakly expressed in the foregut region at NF25-35 (data not shown). In contrast, we detected robust expression of *fgf7, fgf9* and *fgf10* during respiratory induction (NF32-35). *Fgf7* and *fgf10* transcripts were detected in the ventral-lateral plate mesoderm of the foregut with *fgf10* being more broadly expressed (Fig.8A–B'). In contrast, *fgf9* was only detected in the dorsal-lateral mesoderm (Fig. 8C, C').

We also examined all 4 FGF receptors (Fgfr) and found *fgfr1*, *fgfr3*, and *fgfr4* to be ubiquitous expressed throughout the foregut endoderm and lpm (Fig. 8D–F' and data not shown). In contrast, *fgfr2* mRNA was enriched in the ventral foregut endoderm with lower levels in the surrounding lpm (Fig. 8E, E'); a pattern similar to *FgfR2* in the mouse foregut endoderm (Arman et al., 1999). Fgfr tyrosine kinases can activate several intracellular

NIH-PA Author Manuscript

NIH-PA Author Manuscript

NIH-PA Author Manuscript

pathways, and during both mouse and *Xenopus* foregut development the Fgfr-Mapk-Erk1/2 branch has been shown to be functionally important (Calmont et al., 2006; Shifley et al., 2012). To monitor active FGF signaling during respiratory specification stages, we utilized antibodies that detect the phosphorylated active form of Fgfr1 (pFgfr1; Fig. 8G–L) or phosphorylated Erk1/Erk2 (pErk1/2; Fig. 8M–R). Immunofluorescence at NF35 and NF42 revealed pFgfr1 enriched in foregut epithelium cell membranes and strong pErk1/2 staining, in both the ventral and dorsal foregut endoderm, as well as in the surrounding lpm at lower levels. Pharmacological inhibition of FGF receptor tyrosine kinase activity using the small molecule PD173074 (Mohammadi et al., 1998) abolished the pFgfr1 and pErk1/2 signals (data not shown).

Together these data are consistent with findings in mice where multiple FGF ligands and receptors are expressed at the right time and place to regulate early lung development through the Mapk-Erk1/2 pathway. In addition the uniform pFgfr and pErk1/2 that we observe throughout the foregut epithelium suggests that FGF may have a passive role in lung induction and that localized FGF signaling probably cannot account for D–V patterning of the foregut.

Expression of the BMP pathway components during Xenopus respiratory specification

D-V patterning of the mouse foregut into ventral Nkx2.1^{+} and dorsal Sox2^{+} domains is dependent upon a balance of ventrally-produced BMP ligands and the dorsally-produced BMP antagonist Noggin (Fausett and Klingensmith, 2012; Hines and Sun, 2014; Que et al., 2006). We find the same arrangement in the *Xenopus* foregut, with *bmp2*, *bmp4*, and *bmp7* expressed in the ventral lpm and developing heart (Fig. 9A–C'), while *noggin* is exclusively expressed in the notochord (data not shown; Xenbase). Transcripts encoding BMP type I (BMPR1) and BMP type II (BMPR2) receptor genes *bmpr1a*, *bmpr1b* and *bmpr2* were expressed throughout the foregut with transcripts being more abundant in the mesoderm than endoderm (Fig. 9D–F') at NF35.

Ligand binding and activation of the BMPR kinases results in phosphorylation of the intracellular effectors Smad1/5/8 (Smad1), which translocate to the nucleus to regulate BMP-responsive transcription. To determine whether there was differential BMP activity along the D–V axis of the *Xenopus* foregut, we performed immunofluorescence with an antibody that specifically detects pSmad1 (Fig. 9G–L). Staining was performed in *Tg(7xtcf:degpf)* transgenic Tcf/β-catenin reporter embryos allowing us to test whether the presumptive lung epithelium was responding to both the BMP/Smad1 and Wnt/β-catenin pathways at the same time. Nuclear pSmad1 was detected in both the ventral foregut endoderm and ventral lpm, but little if any in the dorsal foregut at NF35 (Fig. 9G–I). The ventral pSmad1 signal coincided with *Tg(7xtcf:degpf)* transgene expression, indicating that β-catenin and Smad1 are active in the same ventral foregut cells. Moreover our analysis indicates that not only is the epithelium responding but that the splanchnic mesoderm, the source of Wnt and BMP ligands, is also responding consistent with a role of these pathways in maturation of the mesenchyme. As a specificity control, inhibition of BMPR1 kinase activity using the small molecule DMH-1 abolished the pSmad1 immunoreactivity (data not shown). At NF42 pSmad1 was obvious in the tracheal endoderm and mesoderm (Fig. 9J),

NIH-PA Author Manuscript

NIH-PA Author Manuscript

NIH-PA Author Manuscript

pSmad1 levels were lower in the two primary bronchi (Fig. 9K), but again robust in the distal tips of the bronchi (Fig. 9L). This is similar to observations in mouse where BMP signaling is essential for developing trachea (Domyan et al., 2011) and regulates proximal-distal patterning of the respiratory system (Hyatt et al., 2002; Weaver et al., 2000).

Together our expression analysis of the Wnt, FGF, and BMP pathway components suggests that the gene regulatory networks controlling D–V foregut pattering and specification of respiratory progenitors are evolutionarily-conserved between *Xenopus* and mammals.

Functional epistasis of the Wnt, FGF and BMP pathways during D–V foregut patterning and respiratory lineage specification

Recent studies have demonstrated that Wnt2/2b and FGF signaling are essential for specification of *Xenopus* respiratory progenitors, while BMP signaling is not absolutely required (Rankin et al., 2012; Shifley et al., 2012; Wang et al., 2011). These experiments also suggested that Wnt acts downstream of FGF signaling, but this remains to be thoroughly tested. Moreover, how the Wnt, FGF and BMP pathways regulate the D–V patterning of the *Xenopus* foregut has not been examined in detail.

To more completely resolve the relative roles of these pathways in *Xenopus* respiratory system development we first systematically compared Wnt, FGF and BMP loss of function by injection of wnt2-MO and wnt2b-MOs (wnt-2/2b-MOs), or treatment of embryos from NF25-34 with PD173047 (PD) or DMH1 to inhibit FGFR and BMPR activity respectively (Mohammadi et al., 1998; Myers and Krieg, 2013). Consistent with previous reports the wnt2/2b-MOs and PD treatment abolished *nkx2.1* mRNA expression while DMH1 treated embryos still expressed *nkx2.1*, albeit at a lower level (Fig. 10A–L). Immunostaining confirmed the absence of Nkx2.1 in Wnt2/2b-depleted foreguts with an expansion of $Sox2^+$ cells into the ventral epithelium (Fig. 10E). FGFR inhibition resulted not only in a loss of Nkx2.1 but also reduced Sox2 and Foxf1 in the dorsal epithelium and splanchnic mesenchyme (Fig. 10B, H), consistent with pERK1/2 activity in these tissues (Fig. 8M–O) and observations that FGF signaling maintains multiple cell fates in the foregut (Deimling and Drysdale, 2011; Rankin et al., 2012). BMP-inhibition resulted in a 45% reduction in the number of $Nkx2.1^+$ cells with a 29% increase in $Sox2^+$ cells ($p < 0.005$ in student t-test, $n = 5$ embryos) that expanded into the ventral region of the foregut (Fig. 10K). Foxf1 staining was also reduced by DMH1 (Fig. 10K) suggesting that BMP signaling also maintains the mesenchyme, consistent with nuclear pSmad1 observed in the $Foxf1^+$ lpm (Fig. 9). In situ hybridization for *sftpc* at NF42 demonstrated that wnt2/2b-MO and PD treated embryos exhibit lung agenesis as expected (Fig. 10C, F, I). In contrast BMP-inhibited embryos still had *sftpc*+ lung buds, although these were smaller than vehicle (DMSO) treated controls (Fig. 10L).

Pharmacological experiments have shown that stabilization of cytosolic β-catenin, by the small molecule BIO, can rescue *nkx2.1* expression in *Xenopus* embryos where FGF signaling has been inhibited (Rankin et al., 2012), suggesting that Wnt acts downstream of FGF. However, these data do not exclude the possibility that FGF and Wnt might act in parallel and that FGF activation might rescue lung development in Wnt-inhibited embryos. To test this we injected RNA encoding an inducible FGFR1 (iFGFR1) into the foregut

NIH-PA Author Manuscript

NIH-PA Author Manuscript

NIH-PA Author Manuscript

region of control and wnt2/2b-MO embryos. Addition of the small molecule AP20187 to the culture media results in receptor clustering and FGFR kinase activation (Pownall et al., 2003; Shifley et al., 2012). As positive controls the direct FGF target gene *sprouty2* (Sivak et al., 2005) and pERK1/2 were only induced upon AP20187 treatment (data not shown). Activation of iFGFR in control embryos at NF25 results in ectopic *nkx2.1* throughout the foregut (Shifley et al., 2012; data not shown), however iFGFR1 activation did not rescue *nkx2.1* or *sftpc* expression in wnt2/2b-MO embryos (Fig. 10M).

To more rigorously test the FGF>Wnt>Nkx2.1 model we injected mRNA encoding an inducible Lef1-β-catenin fusion protein (GR:LefdN-βCTA) (Domingos et al., 2001) into the foregut endoderm of control and FGF-inhibited embryos. This construct has the DNA binding domain of Lef1 fused to the β-catenin transactivation domain. Addition of dexamethasone (dex) to the culture media results in translocation of the GR:LefdN-βCTA to the nucleus where it activates Wnt/β-catenin responsive genes (Domingos et al., 2001; McLin et al., 2007). Dex induction of GR:LefdN-βCTA at NF25 was sufficient to expand and rescue *nkx2.1* and *sftpc* in control embryos and wnt2/2b-MO embryos respectively (Fig. 10P–U). Importantly GR:LefdN-βCTA activation rescued *nkx2.1* and *sftpc* in embryos where FGF-signaling was inhibited (Fig. 10V, W). We conclude from these experiments that Wnt/β-catenin is sufficient to specify respiratory fate downstream of FGF.

Finally we assessed the relationship between Wnt and BMP signaling and found that blocking BMPR activity by DMH1 treatment prevented the ectopic *nkx2.1* and *sftpc* induced by GR:LefdN-βCTA, but similar to BMPR-inhibition alone (Fig. 10J, L) *nkx2.1* and *sftpc* were still expressed in the normal lung domain (Fig. 10X, Y). These results are very similar to genetic studies in mice showing that BMPR signaling is required for ectopic *nkx2.1* caused by activation of β-catenin in the foregut epithelium (Domyan et al., 2011) and suggest that BMP/Smad1 cooperates with Wnt/β-catenin to coordinate D–V foregut patterning and respiratory system development in *Xenopus*.

Conclusions

In this "*Patterns and Phenotypes*" report we present a histological and molecular atlas of early respiratory system development in *Xenopus*, focusing on how the Wnt, FGF and BMP pathways coordinate foregut patterning and specification of the respiratory epithelium. We show that at both the histological and molecular level the early foregut and lung development in *Xenopus* (prior to metamorphosis) is very similar to the embryonic phase of murine foregut and lung development between E8.5-E10.5, before branching morphogenesis.

Our expression analysis identified candidate ligands, receptors and effectors that probably mediate Wnt, BMP, and FGF signaling during respiratory cell fate specification in *Xenopus*, and possibly in mammals as well. Using a combination of loss-of–function and gain-of-function approaches we clarified the role these pathways play in D–V patterning of the *Xenopus* foregut and how these signals coordinate respiratory system development. Together with previous studies our data suggest that multiple FGF ligands acting over an extended period of time promote development of both foregut endoderm and mesoderm lineages (Deimling and Drysdale, 2011; Rankin et al., 2012; Shifley et al., 2012). We rigorously

NIH-PA Author Manuscript

NIH-PA Author Manuscript

NIH-PA Author Manuscript

confirmed that canonical Wnt/β-catenin signaling is sufficient to specify Nkx2.1$^+$ respiratory progenitors downstream of FGF. We also demonstrate that between NF25-35, BMP signaling acts in concert with Wnt/β-catenin to pattern the foregut into ventral Nkx2.1$^+$ trachea and Sox2$^+$ esophagus, which is essentially identical to observation in mice. In summary this work provides the essential groundwork for future research using *Xenopus* to study the conserved gene regulatory networks governing respiratory system development.

Experimental Procedures

Embryo culture, pharmacological treatment, and microinjection

Culture and microinjection of *X. laevis* and *X. tropicalis* embryos was performed as previously described (Sive et al., 2000). Small molecules were dissolved in DMSO or Ethanol according to manufacturer's instructions and working concentrations were as follows: 100 μM PD173074 (Tocris Bioscience), 50 μM XAV939 (Sigma), 20 μM DMH-1 (Sigma). Dexamethasone (1 μM; Sigma D4902) was used to activate the GR-LefdN-BCTA construct (Domingos et al.; McLin et al.) and AP20187 (2 μM; Clontech) was used to activate the iFGFR1 construct (Pownall et al., 2003). Culture buffers were refreshed with the inhibitors or inductive chemicals every 12–16 hours. Morpholino oligos to Wnt2/2b were previously described (Rankin et al., 2012).

Histology, In-situ hybridization, and Immunofluorescence

Standard histological procedures were used for Hematoxylin/Eosin, Alcian Blue, and Mason's trichrome staining of 7 μm paraffin sections. For adult *Xenopus* lung histology, adults were sacrificed by lethal anesthetic, pithed, and the trachea/lung was inflated with fixative prior to removing it from the animal. In-situ hybridization on embryos fixed overnight at 4 C in MEMFA was performed as previously described (Sive et al., 2000). In-situ hybridization on paraffin sections was performed as described (Butler et al., 2001). Plasmid and probe synthesis information is available upon request. Whole mount immunofluorescence was performed on bisected embryos fixed for 1 hour in MEMFA and subsequently post-fixed in Dent's fixative (80%Methanol / 20% DMSO) at −20 C as previously described (Rankin et al., 2012). 10 μm optical sections along the A–P axis were obtained by confocal microscopy, with identical laser settings used for all images of a given experiment.

The following antibodies (company catalog number/ species, type) were used for immunostaining: anti-CSPG (Sigma #C8035 / mouse monoclonal), Anti-EGFP (Clontech #63259 / mouse monoclonal), anti-phospho-ERK1/2-Thr202/Tyr204 (Cell Signaling #9101 / rabbit polyclonal), anti-Fibronectin (clone4H2 DeSimone lab, mouse monoclonal), anti-Foxf1 (R&D systems #AF4798/ goat polyclonal), anti-phospho-Ffgr1-Tyr653 / Tyr 654 (Millipore# 06-1433 /rabbit polyclonal), anti-HSPG (Amsbio- Seikagaku #370260-1 / mouse monoclonal) anti-Laminin alpha 1 (Sigma# L9393 / rabbit poyclonal), anti-Nkx2.1 (Santa cruz# sc-13040 / rabbit polyclonal), anti-Nkx2.1 (Thermo Scientific# MS-699-P1 / mouse monoclonal), anti-phospho-Smad1/5/8 (Cell signaling #9511 / rabbit polyclonal), anti-Sox2 (Abcam #ab97959 / rabbit polyclonal), anti-Sox2 (Abcam #79351 / mouse monoclonal), and anti-p63 (Abcam #ab735). To detect the epitope recognized by the pan-

NIH-PA Author Manuscript

NIH-PA Author Manuscript

NIH-PA Author Manuscript

HSPG antibody, samples were treated with 50u/mL Heparitinase III (sigma#H8891) for 45 minutes at 37 C prior to blocking.

Acknowledgements

We thank members of the “Endoderm club” particular John Shannon, Jim Wells and Kyle McCracken for helpful discussions. We thank Harv Isaacs for the iFGFR1 plasmid and Doug DeSimone for anti-Fibronectin antibodies. M.W. and E.T.S. were supported by T32 HL007752 and T32 HD07463 fellowships respectively. H.T. and K.V. received grants from Interuniversity Attraction Poles IAP7; Foundation against Cancer 2010-162, Research Foundation Flanders G.0942.10N, G.0294.13N. This work was funded by NIH grant HL114898 to A.M.Z.

References

Arman E, Haffner-Krausz R, Gorivodsky M, Lonai P. Fgfr2 is required for limb outgrowth and lung-branching morphogenesis. Proceedings of the National Academy of Sciences of the United States of America. 1999; 96:11895–11899. [PubMed: 10518547]

Bartel H, Lametschwandtner A. Intussusceptive microvascular growth in the lung of larval Xenopus laevis Daudin: a light microscope, transmission electron microscope and SEM study of microvascular corrosion casts. Anat Embryol (Berl). 2000; 202:55–65. [PubMed: 10926096]

Bell SM, Schreiner CM, Wert SE, Mucenski ML, Scott WJ, Whitsett JA. R-spondin 2 is required for normal laryngeal-tracheal, lung and limb morphogenesis. Development. 2008; 135:1049–1058. [PubMed: 18256198]

Blitz IL, Andelfinger G, Horb ME. Germ layers to organs: using Xenopus to study “later” development. Semin Cell Dev Biol. 2006; 17:133–145. [PubMed: 16337415]

Butler K, Zorn AM, Gurdon JB. Nonradioactive in situ hybridization to xenopus tissue sections. Methods. 2001; 23:303–312. [PubMed: 11316431]

Calmont A, Wandzioch E, Tremblay KD, Minowada G, Kaestner KH, Martin GR, Zaret KS. An FGF response pathway that mediates hepatic gene induction in embryonic endoderm cells. Dev Cell. 2006; 11:339–348. [PubMed: 16950125]

Chang DR, Martinez Alanis D, Miller RK, Ji H, Akiyama H, McCrea PD, Chen J. Lung epithelial branching program antagonizes alveolar differentiation. Proc Natl Acad Sci U S A. 2013; 110:18042–18051. [PubMed: 24058167]

Deimling SJ, Drysdale TA. Fgf is required to regulate anterior-posterior patterning in the Xenopus lateral plate mesoderm. Mechanisms of development. 2011; 128:327–341. [PubMed: 21763769]

Domingos PM, Itasaki N, Jones CM, Mercurio S, Sargent MG, Smith JC, Krumlauf R. The Wnt/beta-catenin pathway posteriorizes neural tissue in Xenopus by an indirect mechanism requiring FGF signalling. Dev Biol. 2001; 239:148–160. [PubMed: 11784025]

Domyan ET, Ferretti E, Throckmorton K, Mishina Y, Nicolis SK, Sun X. Signaling through BMP receptors promotes respiratory identity in the foregut via repression of Sox2. Development. 2011; 138:971–981. [PubMed: 21303850]

Fausett SR, Klingensmith J. Compartmentalization of the foregut tube: developmental origins of the trachea and esophagus. Wiley interdisciplinary reviews. Developmental biology. 2012; 1:184–202. [PubMed: 23801435]

Feder ME, Seale DB, Boraas ME, Wassersug RJ, Gibbs AG. Functional conflicts between feeding and gas exchange in suspension-feeding tadpoles, Xenopus laevis. J Exp Biol. 1984; 110:91–98. [PubMed: 6747542]

Goss AM, Tian Y, Cheng L, Yang J, Zhou D, Cohen ED, Morrisey EE. Wnt2 signaling is necessary and sufficient to activate the airway smooth muscle program in the lung by regulating myocardin/Mrtf-B and Fgf10 expression. Dev Biol. 2011; 356:541–552. [PubMed: 21704027]

Goss AM, Tian Y, Tsukiyama T, Cohen ED, Zhou D, Lu MM, Yamaguchi TP, Morrisey EE. Wnt2/2b and beta-catenin signaling are necessary and sufficient to specify lung progenitors in the foregut. Dev Cell. 2009; 17:290–298. [PubMed: 19686689]

Harland RM, Grainger RM. Xenopus research: metamorphosed by genetics and genomics. Trends Genet. 2011; 27:507–515. [PubMed: 21963197]

NIH-PA Author Manuscript NIH-PA Author Manuscript NIH-PA Author Manuscript

Harris-Johnson KS, Domyan ET, Vezina CM, Sun X. beta-Catenin promotes respiratory progenitor identity in mouse foregut. Proc Natl Acad Sci U S A. 2009; 106:16287–16292. [PubMed: 19805295]

Herriges M, Morrisey EE. Lung development: orchestrating the generation and regeneration of a complex organ. Development. 2014; 141:502–513. [PubMed: 24449833]

Hines EA, Sun X. Tissue Crosstalk in Lung Development. J Cell Biochem. 2014

Hollemann T, Pieler T. Xnkx-2.1: a homeobox gene expressed during early forebrain, lung and thyroid development in Xenopus laevis. Dev Genes Evol. 2000; 210:579–581. [PubMed: 11180810]

Huang SX, Islam MN, O'Neill J, Hu Z, Yang YG, Chen YW, Mumau M, Green MD, Vunjak-Novakovic G, Bhattacharya J, Snoeck HW. Efficient generation of lung and airway epithelial cells from human pluripotent stem cells. Nat Biotechnol. 2014; 32:84–91. [PubMed: 24291815]

Hyatt BA, Resnik ER, Johnson NS, Lohr JL, Cornfield DN. Lung specific developmental expression of the Xenopus laevis surfactant protein C and B genes. Gene Expr Patterns. 2007; 7:8–14. [PubMed: 16798105]

Hyatt BA, Shangguan X, Shannon JM. BMP4 modulates fibroblast growth factor-mediated induction of proximal and distal lung differentiation in mouse embryonic tracheal epithelium in mesenchyme-free culture. Developmental dynamics : an official publication of the American Association of Anatomists. 2002; 225:153–165. [PubMed: 12242715]

Kalinichenko VV, Zhou Y, Bhattacharyya D, Kim W, Shin B, Bambal K, Costa RH. Haploinsufficiency of the mouse Forkhead Box f1 gene causes defects in gall bladder development. J Biol Chem. 2002; 277:12369–12374. [PubMed: 11809759]

Lazzaro D, Price M, de Felice M, Di Lauro R. The transcription factor TTF-1 is expressed at the onset of thyroid and lung morphogenesis and in restricted regions of the foetal brain. Development. 1991; 113:1093–1104. [PubMed: 1811929]

Lea R, Papalopulu N, Amaya E, Dorey K. Temporal and spatial expression of FGF ligands and receptors during Xenopus development. Developmental dynamics : an official publication of the American Association of Anatomists. 2009; 238:1467–1479. [PubMed: 19322767]

Longmire TA, Ikonomou L, Hawkins F, Christodoulou C, Cao Y, Jean JC, Kwok LW, Mou H, Rajagopal J, Shen SS, Dowton AA, Serra M, Weiss DJ, Green MD, Snoeck HW, Ramirez MI, Kotton DN. Efficient derivation of purified lung and thyroid progenitors from embryonic stem cells. Cell Stem Cell. 2012; 10:398–411. [PubMed: 22482505]

Maeda Y, Dave V, Whitsett JA. Transcriptional control of lung morphogenesis. Physiol Rev. 2007; 87:219–244. [PubMed: 17237346]

Mahlapuu M, Enerback S, Carlsson P. Haploinsufficiency of the forkhead gene Foxf1, a target for sonic hedgehog signaling, causes lung and foregut malformations. Development. 2001; 128:2397–2406. [PubMed: 11493558]

Matsumoto K, Yoshitomi H, Rossant J, Zaret KS. Liver organogenesis promoted by endothelial cells prior to vascular function. Science. 2001; 294:559–563. [PubMed: 11577199]

McLin VA, Rankin SA, Zorn AM. Repression of Wnt/{beta}-catenin signaling in the anterior endoderm is essential for liver and pancreas development. Development. 2007; 134:2207–2217. [PubMed: 17507400]

Meban C. The pneumonocytes in the lung of Xenopus laevis. J Anat. 1973; 114:235–244. [PubMed: 4352575]

Mohammadi M, Froum S, Hamby JM, Schroeder MC, Panek RL, Lu GH, Eliseenkova AV, Green D, Schlessinger J, Hubbard SR. Crystal structure of an angiogenesis inhibitor bound to the FGF receptor tyrosine kinase domain. EMBO Journal. 1998; 17:5896–5904. [PubMed: 9774334]

Morrisey EE, Hogan BL. Preparing for the first breath: genetic and cellular mechanisms in lung development. Developmental cell. 2010; 18:8–23. [PubMed: 20152174]

Myers CT, Krieg PA. BMP-mediated specification of the erythroid lineage suppresses endothelial development in blood island precursors. Blood. 2013; 122:3929–3939. [PubMed: 24100450]

Niehrs C. The complex world of WNT receptor signalling. Nat Rev Mol Cell Biol. 2012; 13:767–779. [PubMed: 23151663]

NIH-PA Author Manuscript NIH-PA Author Manuscript NIH-PA Author Manuscript

Nieuwkoop, PD.; Faber, J. Normal table of Xenopus laevis (Daudin): a systematical and chronological survey of the development from the fertilized egg till the end of metamorphosis. New York: Garland Publishing, Inc; 1994.

Okada Y, Ishiko S, Daido S, Kim J, Ikeda S. Comparative morphology of the lung with special reference to the alveolar epithelial cells. I. Lung of the amphibia. Acta tuberculosea Japonica. 1962; 11:63–72. [PubMed: 13939767]

Ornitz DM, Yin Y. Signaling networks regulating development of the lower respiratory tract. Cold Spring Harb Perspect Biol. 2012; 4

Pownall ME, Welm BE, Freeman KW, Spencer DM, Rosen JM, Isaacs HV. An inducible system for the study of FGF signalling in early amphibian development. Dev Biol. 2003; 256:89–99. [PubMed: 12654294]

Que J, Choi M, Ziel JW, Klingensmith J, Hogan BL. Morphogenesis of the trachea and esophagus: current players and new roles for noggin and Bmps. Differentiation. 2006; 74:422–437. [PubMed: 16916379]

Rankin SA, Gallas AL, Neto A, Gomez-Skarmeta JL, Zorn AM. Suppression of Bmp4 signaling by the zinc-finger repressors Osr1 and Osr2 is required for Wnt/beta-catenin-mediated lung specification in Xenopus. Development. 2012; 139:3010–3020. [PubMed: 22791896]

Rose CS, James B. Plasticity of lung development in the amphibian, Xenopus laevis. Biology open. 2013; 2:1324–1335. [PubMed: 24337117]

Sekine K, Ohuchi H, Fujiwara M, Yamasaki M, Yoshizawa T, Sato T, Yagishita N, Matsui D, Koga Y, Itoh N, Kato S. Fgf10 is essential for limb and lung formation. Nature genetics. 1999; 21:138–141. [PubMed: 9916808]

Serls AE, Doherty S, Parvatiyar P, Wells JM, Deutsch GH. Different thresholds of fibroblast growth factors pattern the ventral foregut into liver and lung. Development. 2005; 132:35–47. [PubMed: 15576401]

Shannon JM, McCormick-Shannon K, Burhans MS, Shangguan X, Srivastava K, Hyatt BA. Chondroitin sulfate proteoglycans are required for lung growth and morphogenesis in vitro. American journal of physiology. Lung cellular and molecular physiology. 2003; 285:L1323–L1336. [PubMed: 12922982]

Shifley ET, Kenny AP, Rankin SA, Zorn AM. Prolonged FGF signaling is necessary for lung and liver induction in Xenopus. BMC Dev Biol. 2012; 12:27. [PubMed: 22988910]

Sivak JM, Petersen LF, Amaya E. FGF signal interpretation is directed by Sprouty and Spred proteins during mesoderm formation. Dev Cell. 2005; 8:689–701. [PubMed: 15866160]

Sive, HL.; Grainger, RM.; Harland, RM. Early Development of Xenopus laevis: A Laboratory Manual. Cold Spring Harbor, NY: Cold Spring Harbor Laboratory Press; 2000.

Small EM, Vokes SA, Garriock RJ, Li D, Krieg PA. Developmental expression of the Xenopus Nkx2-1 and Nkx2-4 genes. Mech Dev. 2000; 96:259–262. [PubMed: 10960795]

Smith DG, Rapson L. Differences in pulmonary microvascular anatomy between Bufo marinus and Xenopus laevis. Cell Tissue Res. 1977; 178:1–15. [PubMed: 402217]

Tran HT, Sekkali B, Van Imschoot G, Janssens S, Vleminckx K. Wnt/beta-catenin signaling is involved in the induction and maintenance of primitive hematopoiesis in the vertebrate embryo. Proc Natl Acad Sci U S A. 2010; 107:16160–16165. [PubMed: 20805504]

Tseng HT, Shah R, Jamrich M. Function and regulation of FoxF1 during Xenopus gut development. Development. 2004; 131:3637–3647. [PubMed: 15229177]

Wang JH, Deimling SJ, D'Alessandro NE, Zhao L, Possmayer F, Drysdale TA. Retinoic acid is a key regulatory switch determining the difference between lung and thyroid fates in Xenopus laevis. BMC developmental biology. 2011; 11:75. [PubMed: 22185339]

Waterman FA. 1939 The origin and development of the internal musculature of the frog lung (Rana pipiens).

Weaver M, Dunn NR, Hogan BL. Bmp4 and Fgf10 play opposing roles during lung bud morphogenesis. Development. 2000; 127:2695–2704. [PubMed: 10821767]

Wert SE, Glasser SW, Korfhagen TR, Whitsett JA. Transcriptional elements from the human SP-C gene direct expression in the primordial respiratory epithelium of transgenic mice. Dev Biol. 1993; 156:426–443. [PubMed: 8462742]

NIH-PA Author Manuscript

NIH-PA Author Manuscript

NIH-PA Author Manuscript

Whitsett JA, Haitchi HM, Maeda Y. Intersections between pulmonary development and disease. Am J Respir Crit Care Med. 2011; 184:401–406. [PubMed: 21642246]

Wiechmann, AF.; Wirsig-Wiechmann, CE. Color atlas of Xenopus laevis histology. Boston: Kluwer Academic Publishers; 2003.

Wong AP, Rossant J. Generation of Lung Epithelium from Pluripotent Stem Cells. Current pathobiology reports. 2013; 1:137–145. [PubMed: 23662247]

Yin A, Winata CL, Korzh S, Korzh V, Gong Z. Expression of components of Wnt and Hedgehog pathways in different tissue layers during lung development in Xenopus laevis. Gene Expr Patterns. 2010; 10:338–344. [PubMed: 20682360]

Yin Y, Wang F, Ornitz DM. Mesothelial- and epithelial-derived FGF9 have distinct functions in the regulation of lung development. Development. 2011; 138:3169–3177. [PubMed: 21750028]

Yin Y, White AC, Huh SH, Hilton MJ, Kanazawa H, Long F, Ornitz DM. An FGF-WNT gene regulatory network controls lung mesenchyme development. Dev Biol. 2008; 319:426–436. [PubMed: 18533146]

Zaret KS, Carroll JS. Pioneer transcription factors: establishing competence for gene expression. Genes Dev. 2011; 25:2227–2241. [PubMed: 22056668]

Zhang B, Tran U, Wessely O. Expression of Wnt signaling components during Xenopus pronephros development. PLoS One. 2011; 6:e26533. [PubMed: 22028899]

NIH-PA Author Manuscript
NIH-PA Author Manuscript
NIH-PA Author Manuscript

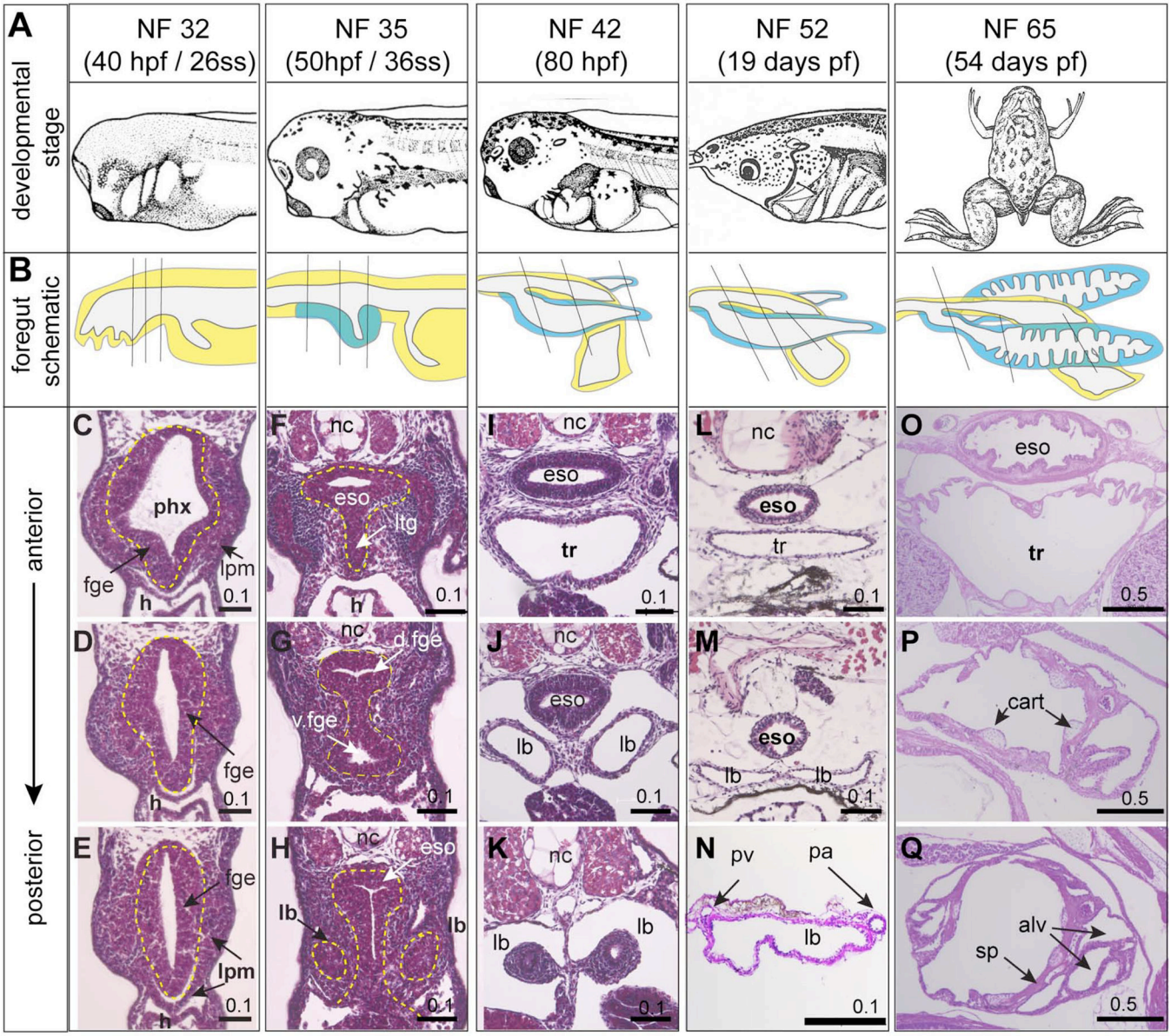

Figure 1. Histology of the developing *Xenopus laevis* foregut and respiratory system

(A) *Xenopus laevis* embryos images at different developmental stages from Nieuwkoop and Faber (1994). **(B)** Schematic illustrations of the foregut region of the embryo at the indicated developmental stages. Endoderm is yellow and respiratory endoderm is blue. **(C–Q)** H&E stained sections of the developing foregut / respiratory system / lungs at the indicated stages; plane of section is indicated in **(B)** and endoderm is outlined by dashed yellow line in C–H. Abbreviations: alv, alveolar sac; cart, cartilage; eso, esophagus; fge, foregut endoderm; h, heart; lb, lung bud; lpm, lateral plate mesosderm; ltg, laryngo-tracheal groove nc, notochord; pa, pulmonary artery; phx, pharynx; pv, pulmonary vein; sp, septae; tr, trachea. Scale bar = 0.1 mm or 0.5 mm as indicated.

NIH-PA Author Manuscript
NIH-PA Author Manuscript
NIH-PA Author Manuscript

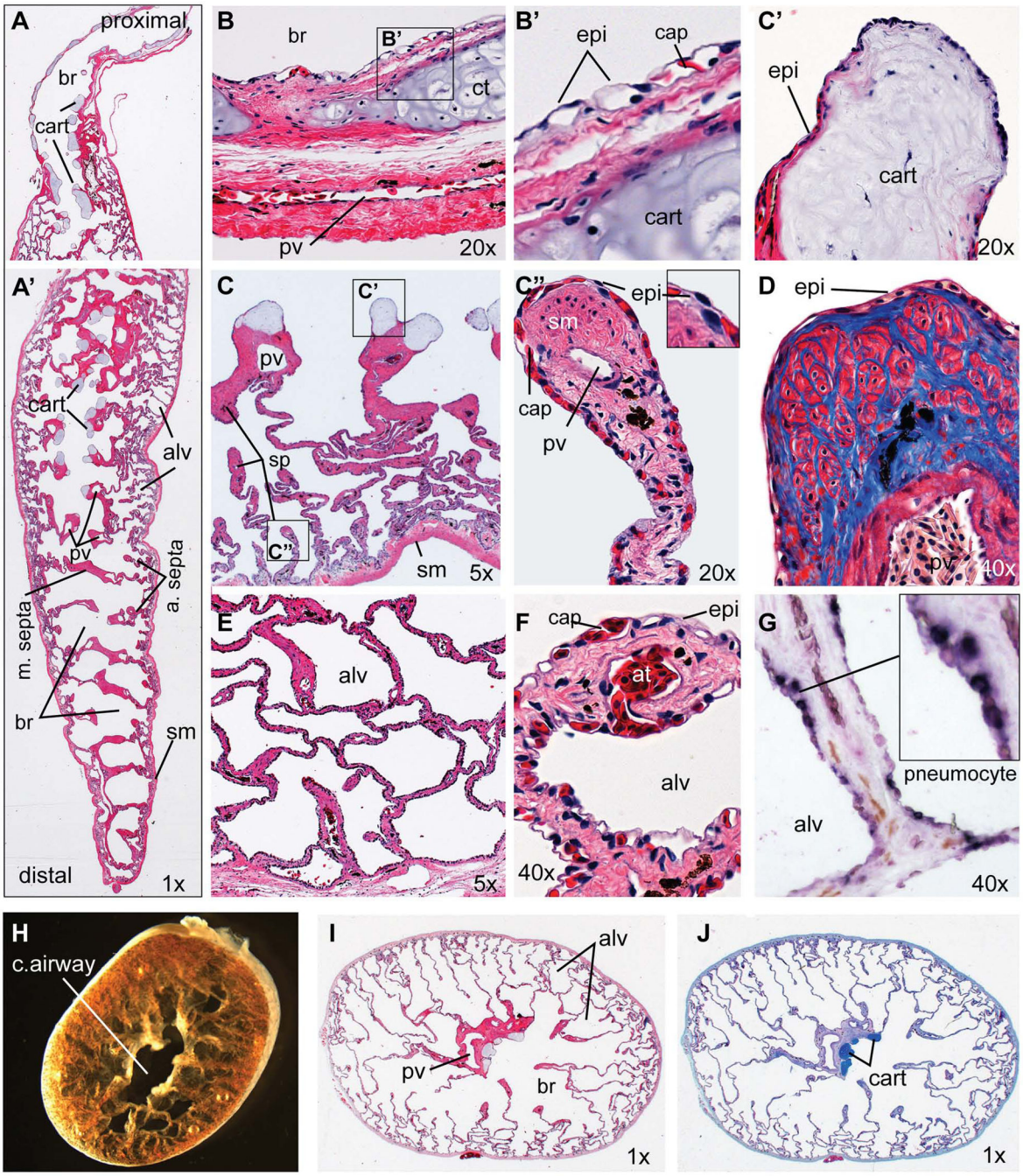

Figure 2. Histology of the adult *Xenopus laevis* lung

(A–G) Longitudinal sections of an adult *Xenopus laevis* lung including **(A)** the proximal and **(A')** distal regions. **(B)** 20X view of proximal main bronchi showing the epithelial lining and bronchi walls with cartilage plate surrounded by layers of smooth muscle and connective tissue containing a major blood vessel. **(B')** Detail view of boxed area in (B) showing the epithelial cells in close apposition to capillaries. **(C)** 5X view of the proximal lung showing major septa containing a pulmonary vein and terminal cartilage nodules with smaller septa forming alveoli. (**C'**) 20X view of a cartilage nodule at the end of the major septa. (**C"**) 20X

NIH-PA Author Manuscript

NIH-PA Author Manuscript

NIH-PA Author Manuscript

view showing the tip of an alveolar septa. **(D)** 40X view of an alveolar septa tip stained with Mason's Trichrome showing collagen fibers (blue) and muscle fibers (red). **(E)** 5X view of smaller alveoli at the lung periphery. **(F)** 40X view of the blood-air interface in the small alveolar walls. **(G)** In-situ hybridization of *sftpc* (dark purple staining) showing expression in epithelial pneumocytes. **(H)** Brightfield of the adult *Xenopus* lung (distal portion) cut in a transverse plane immediately after dissection. **(I)** H&E-stained and **(J)** Alcian blue-stained transverse sections Abbreviations: alv, alveolar space; at, arteriole; br, bronchiolar space; cap, capillary; cart, cartilage; epi, epithelial cell; pv, pulmonary vein; sm, smooth muscle; sp, septae.

NIH-PA Author Manuscript
NIH-PA Author Manuscript
NIH-PA Author Manuscript

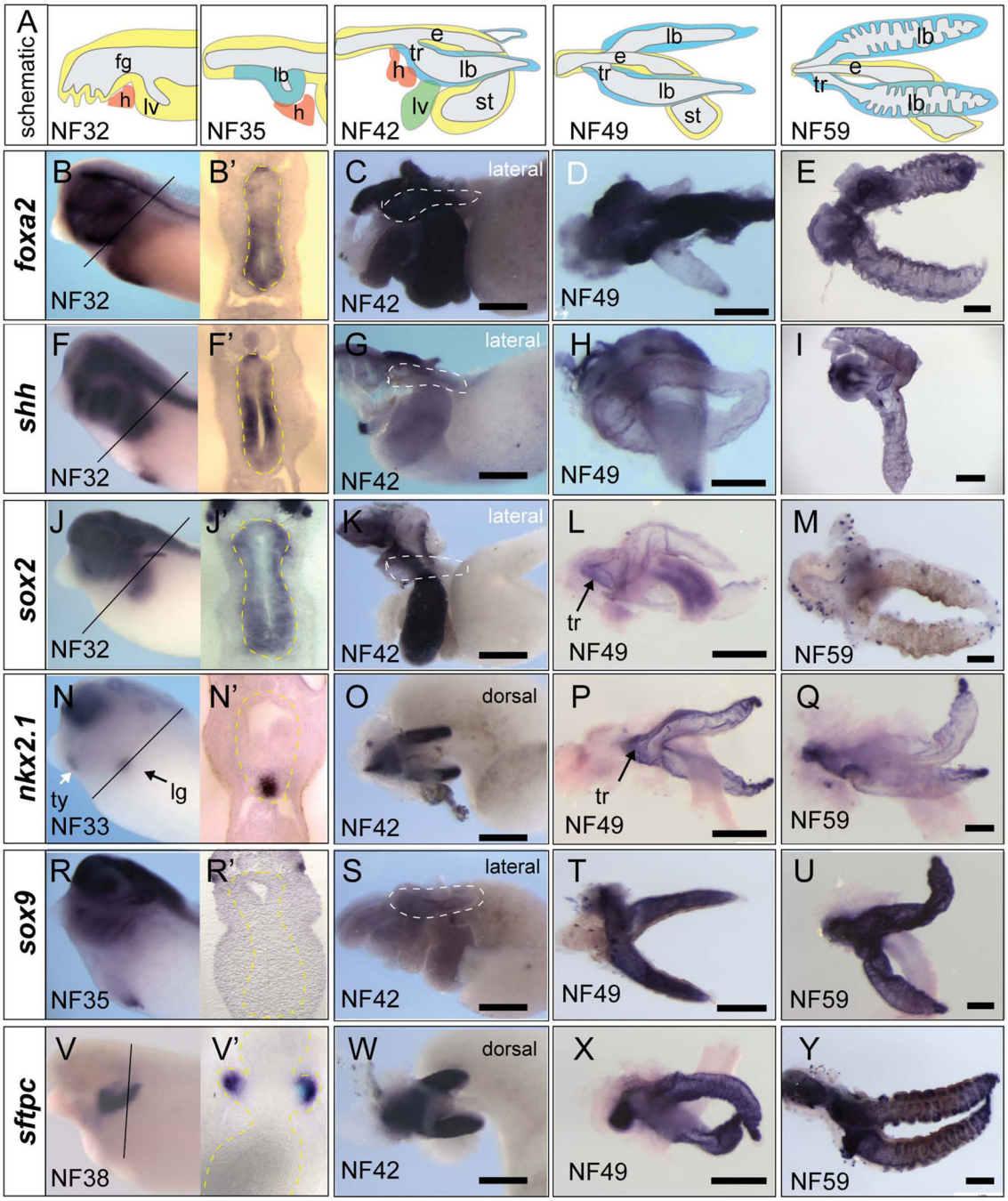

Figure 3. Molecular characterization of the developing *Xenopus* foregut and respiratory epithelium

(**A**). Schematic of the developing foregut region and respiratory system at the indicated developmental stages, with endoderm in yellow, heart (h) in orange, and respiratory epithelium in blue. (**B-Y**) Whole mount in situ hybridization with the indicated probes to whole embryos at NF32 (B, F, J), NF33 (N), NF35 (R), NF38 (V) or to isolated guts at NF42 (C, G, K, O, S, W) or to lung/tracheal/esophageal regions dissected at NF49 (D, H, L,

P, T, X) or NF59 (E, I, M, Q, U, Y). Abbreviations: e, esophagus; fg, foregut; h, heart; lb, lung bud; lg, lung; lv, liver; st, stomach; tr, trachea; ty, thyroid. Scale bar = 0.5 mm

NIH-PA Author Manuscript
NIH-PA Author Manuscript
NIH-PA Author Manuscript

NIH-PA Author Manuscript
NIH-PA Author Manuscript
NIH-PA Author Manuscript

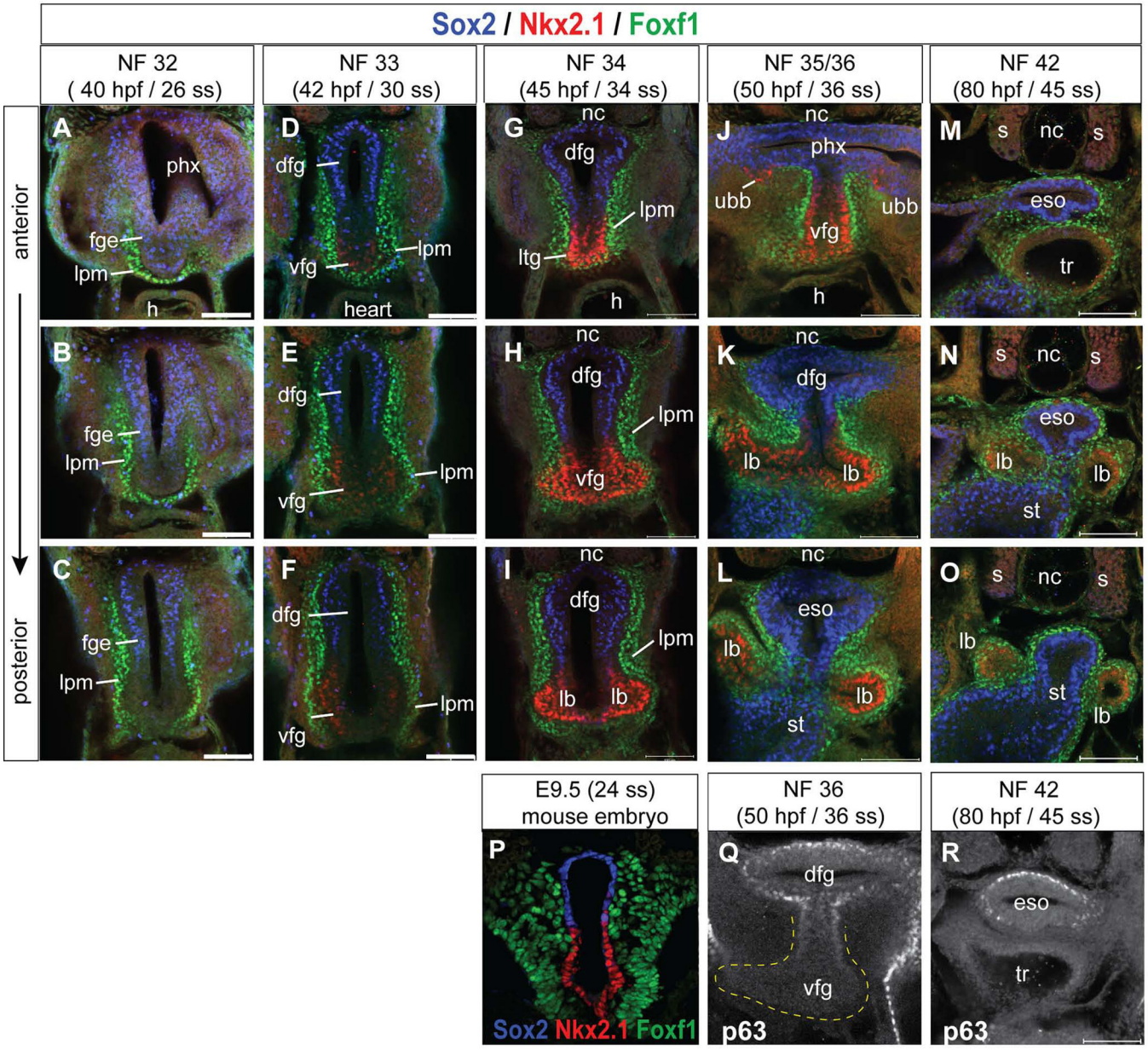

Figure 4. Immunofluorescence analysis of D–V foregut patterning and tracheaesophagus separation in *Xenopus*

(A–O) Confocal immunostaining of the *Xenopus* foregut showing transverse sections at three positions along the anterior-posterior axis at the indicated stages showing protein expression of Sox2 (blue), Nkx2.1 (red), and FoxF1 (green). **(P)** Transverse section through the E9.5 mouse foregut showing similar expression of Sox2 (blue) Nkx2.1 (red) and FoxF1 (green). **(Q, R)** Transverse sections of the *Xenopus* foregut at NF36 and NF42 showing P63 expression (white) in the dorsal foregut **(Q)** and esophagus **(R)**. Abbreviations: dfg, dorsal foregut; eso, esophagus; fge, foregut epithelium; h, heart; lb, lung bud; lpm, lateral plate mesoderm; nc, notochord; s, somite; st, stomach; tr, trachea; ubb, ultimobrachial body; vfg, ventral foregut. Scale bar = 0.1 mm.

NIH-PA Author Manuscript
NIH-PA Author Manuscript
NIH-PA Author Manuscript

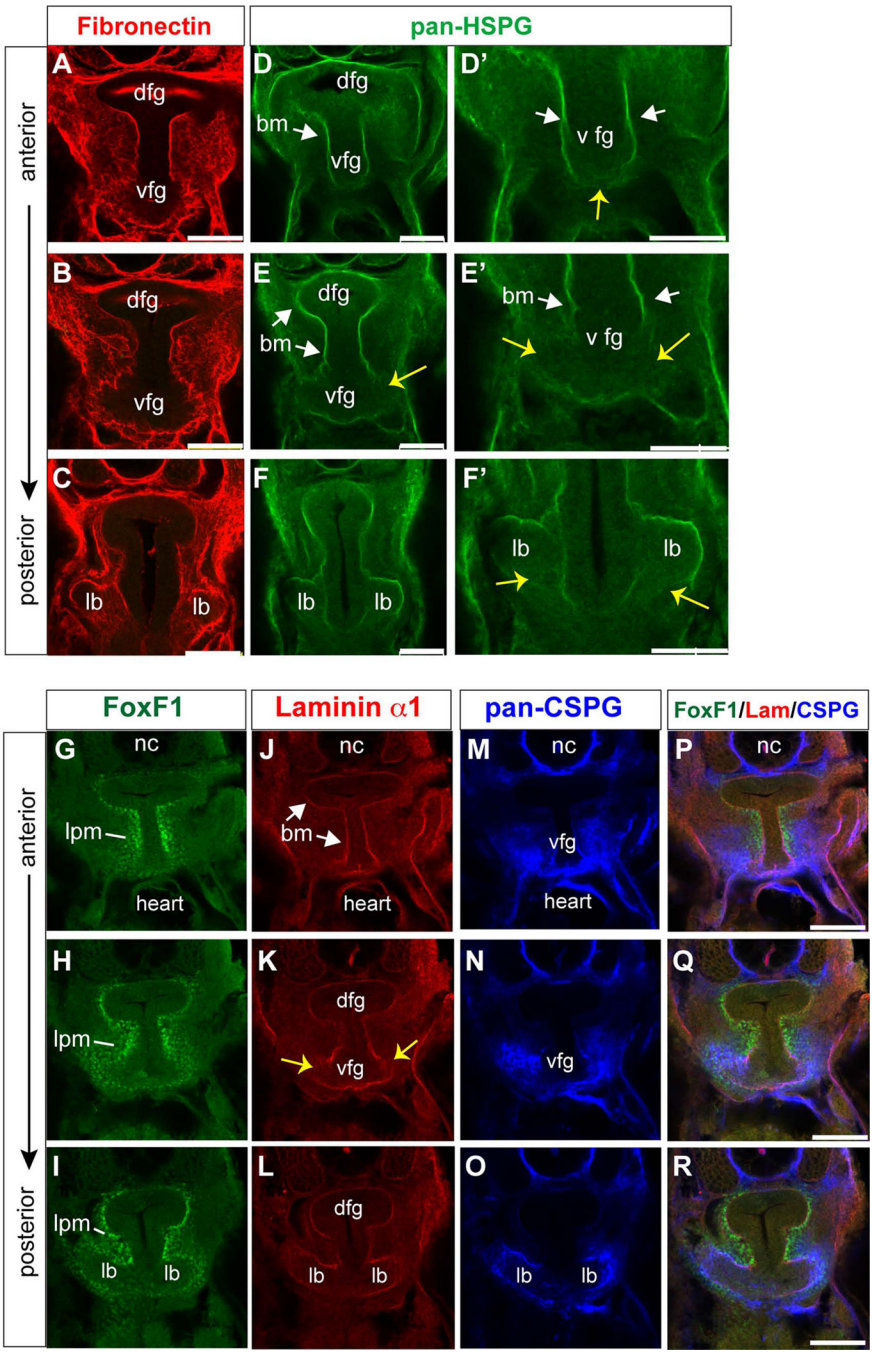

Figure 5. Immunofluorescence analysis of the extracellular matrix and basement membrane surrounding the *Xenopus* foregut and lung buds

(**A-R**) Confocal immunostaining of transverse sections through the NF35 *Xenopus* foregut at three positions along the anterior-posterior axis showing protein expression of **(A–C)** Fibronectin, **(D-F')** Heparin sulfate proteoglycans, **(G–I)** FoxF1, **(J–L)** Laminin alpha-1, and **(M–O)** Chondroitin sulfate proteoglycans. Abbreviations: bm, basement membrane; dfg, dorsal foregut; lb, lung bud; lpm, lateral plate mesoderm; vfg, ventral foregut. Scale bar = 0.1 mm.

NIH-PA Author Manuscript
NIH-PA Author Manuscript
NIH-PA Author Manuscript

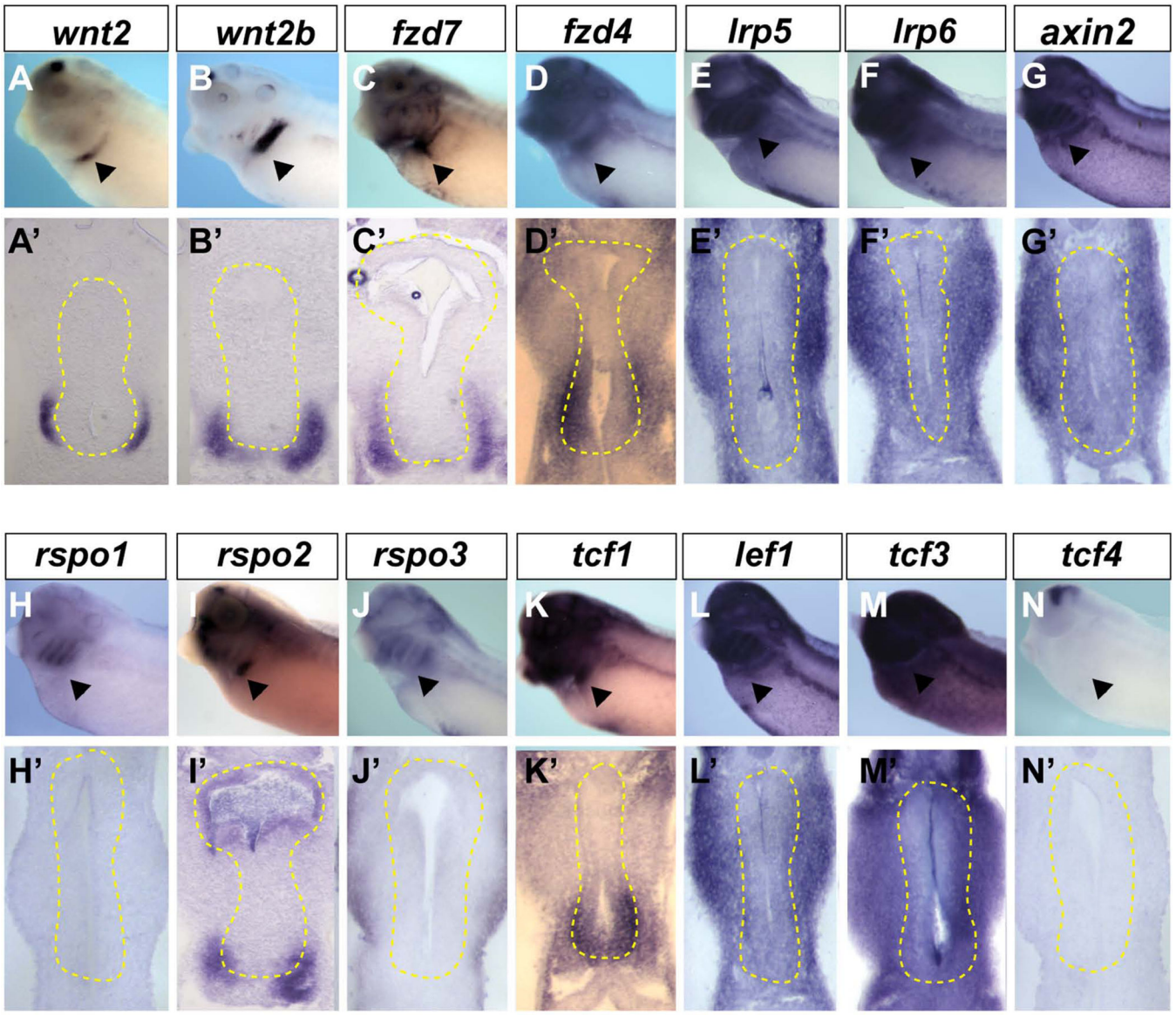

Figure 6. Expression of Wnt pathway components in the *Xenopus* foregut

(A–N) In-situ hybridization using indicated probes to NF34/35 embryos and (**A'-N'**) vibratome sections through the foregut with endoderm outlined by the yellow dashed line. The arrowhead indicates the presumptive lung region.

NIH-PA Author Manuscript
NIH-PA Author Manuscript
NIH-PA Author Manuscript

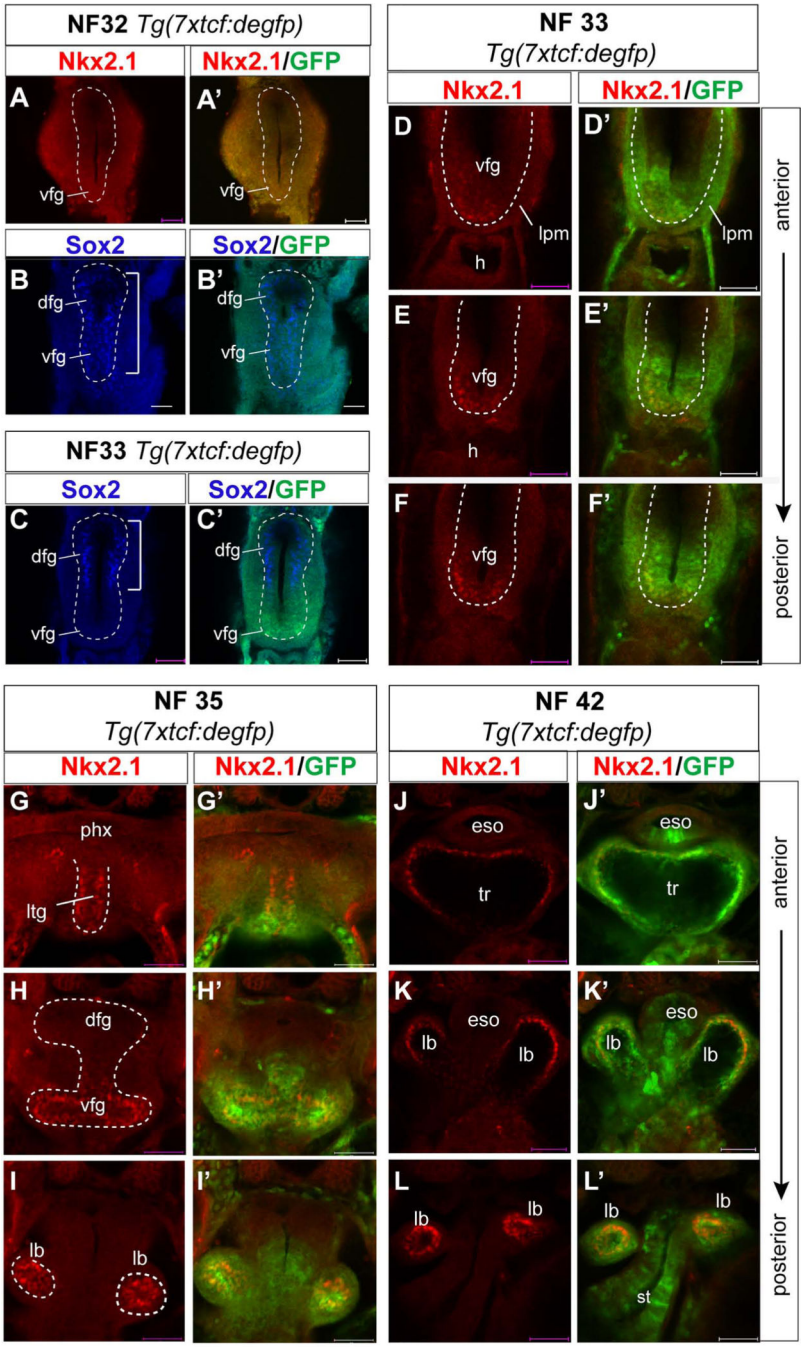

Figure 7. Activity of the canonical Wnt signaling pathway in the *Xenopus* foregut

(A-L') Confocal immunostaining of *Tg(7xtcf:degfp)* transgenic *Xenopus tropicalis* embryos, which express destabilized enhanced GFP in cell responding to Wnt/β-catenin signaling. Transverse sections show protein expression of Nkx2.1 (red) or Sox2 (blue) and eGFP (green) in the foregut at NF32 (A-B'), NF33 (C–E), NF35 (G–I) and NF42 (J–L). EGFP expression is first detected in the ventral foregut at NF32 prior to Nkx2.1 (A'). By NF33 Nkx2.1 is activated and the Sox2 expression domain (white bracket) becomes down regulated (B-C') in the EGFP expressing ventral endoderm. Abbreviations: dfg, dorsal

foregut endoderm; eso, esophagus; lb, lung bud; lpm, lateral plate mesoderm; ltg, laryngo-tracheal grove; st, stomach; tr, trachea; vfg, ventral foregut endoderm. Scale bar = 0.1 mm.

NIH-PA Author Manuscript
NIH-PA Author Manuscript
NIH-PA Author Manuscript

NIH-PA Author Manuscript
NIH-PA Author Manuscript
NIH-PA Author Manuscript

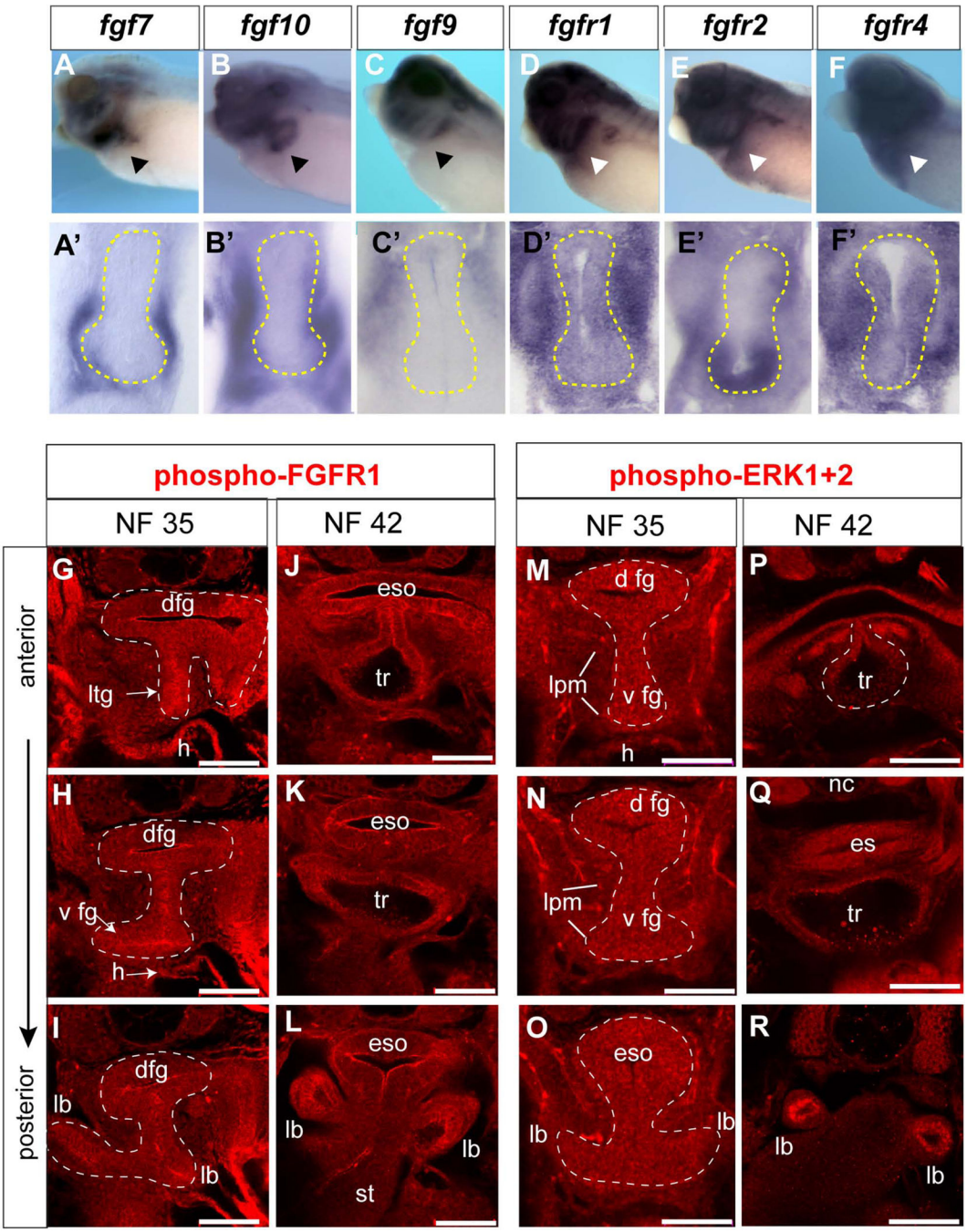

Figure 8. Expression of FGF pathway components in the *Xenopus* foregut

(A–F) In-situ hybridization using indicated probes to NF34/35 embryos and (**A'-F'**) vibratome sections through the foregut with endoderm outlined by the yellow dashed line. **(G–R)** Confocal immunostaining of phosphorylated FGFR1. (**G-L**) and phosphorylated ERK1/2 (**M-R**) in the foregut at the indicated stages. Abbreviations: dfg, dorsal foregut; eso, esophagus; h, heart; lb, lung bud; lpm, lateral plate mesoderm; ltg, laryngo-tracheal groove; st, stomach; tr, trachea.

NIH-PA Author Manuscript
NIH-PA Author Manuscript
NIH-PA Author Manuscript

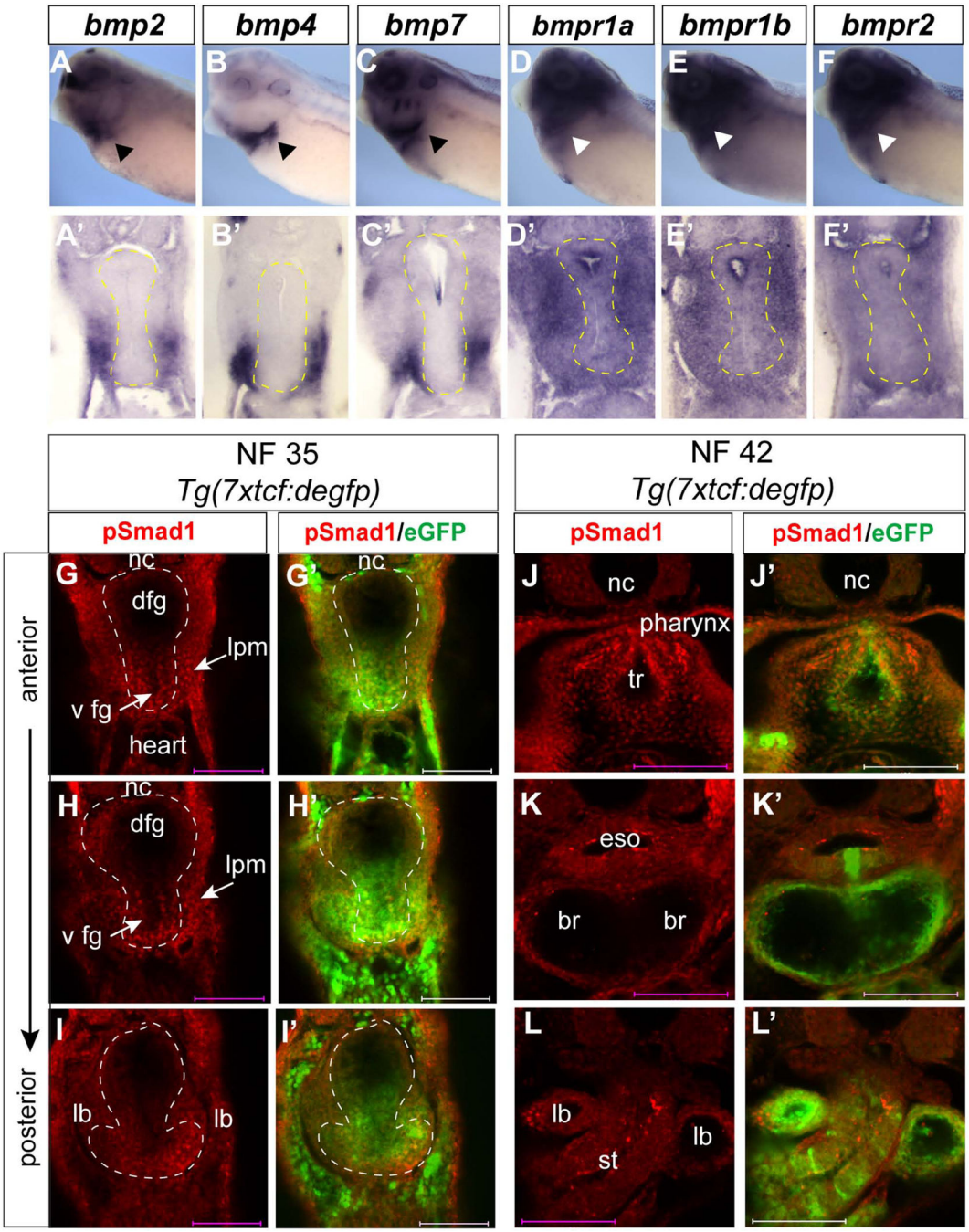

Figure 9. Expression of BMP pathways components in the *Xenopus* foregut

(A–F) In-situ hybridization using indicated probes to NF34/35 embryos and (**A'-F'**) vibratome sections through the foregut with endoderm outlined by the yellow dashed line. **(G-L')** Confocal immunostaining of pSmad1 (red) and eGFP (green) in the foregut of *Tg(7xtcf:degfp)* transgenic *Xenopus tropicalis* embryos at NF35 (G–I) and NF42 (J–L). Abbreviations: br, primary bronchi; dfg, dorsal foregut endoderm; eso, esophagus; lb, lung bud; lpm, lateral plate mesoderm; ltg, laryngo-tracheal grove; st, stomach; tr, trachea; vfg, ventral foregut endoderm.

NIH-PA Author Manuscript
NIH-PA Author Manuscript
NIH-PA Author Manuscript

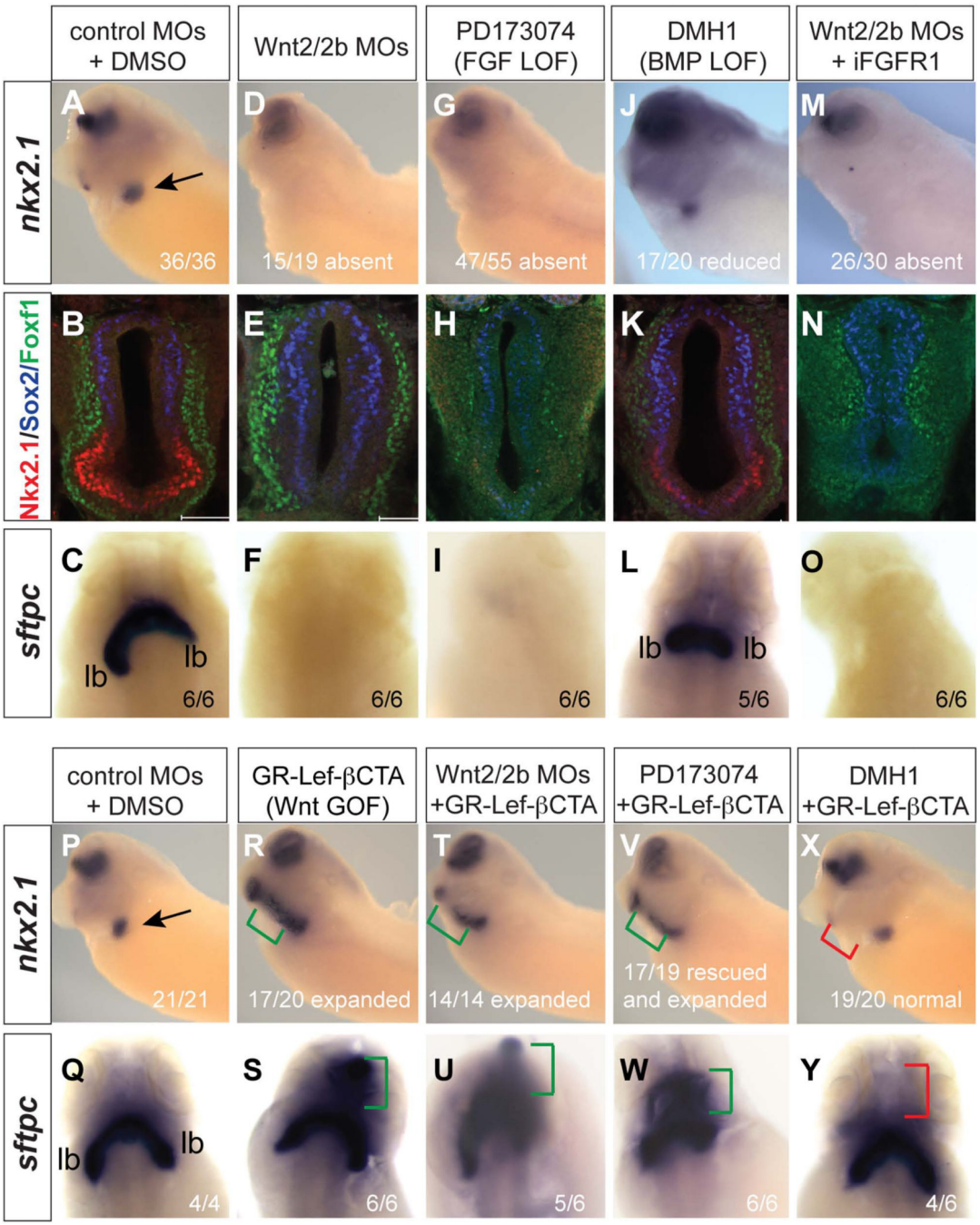

Figure 10. Functional epistasis of Wnt/β-catenin, FGF, and BMP pathways

(A–O) Wnt/β-catenin is necessary and sufficient downstream of FGF to induce respiratory fate. Embryos were injected at the 4-cell stage in both dorsal anterior blastomeres with control-MOs or wnt2/2b-MOs (10 ng/blastomere) and then injected at the 8-cell stage dorsal-vegetally with 800 pg iFGFR1 mRNA (400 pg/blastomere). Subsequently embryos were treated from stages NF25-35 with either, DMSO, PD173074 (100 μM), DMH1 (20 μM), or AP20187 (2 μM to induce the iFGFR1 construct activity). Embryos were analyzed at NF34/35 by in-situ hybridization for *nkx2.1* expression (A, D, G, J, and M)

NIH-PA Author Manuscript

NIH-PA Author Manuscript

NIH-PA Author Manuscript

or by for Nkx2.1 (red), Sox2 (blue), and FoxF1 (green) (B, E, H, K, N). At NF42 siblings were analyzed by in-situ hybridization for *sftpc* expression (C, F, I, L, O). **(P–Y) The expansion of respiratory fate by Wnt/β-catenin requires BMP signaling**. Embryos were injected at the 4-cell stage in both dorsal-anterior blastomeres with control-MOs or wnt2/2b-MOs (10 ng/blastomere) and then injected at the 8-cell stage dorsal-vegetally with 800pg GR-LefdN-BCTA mRNA (400 pg/blastomere). Subsequently the embryos were treated with DMSO, DMH-1, or PD173047 from NF25-35, and then with dex from NF28-35 and analyzed by in-situ hybridization for *nkx2.1* at NF35 (P, R, T, V, X) and *sftpc* at NF42 (Q, S, U, W, Y).